Synthesis of New Polymers Possessing Dense Triazole Backbone by Copper(I)-Catalyzed Azide–Alkyne Cycloaddition

A Doctoral Thesis

by

XU LINLIN

Acknowledgement

This work was carried out under the supervision of Professor Akihito Hashidzume at the Department of Macromolecular Science, Graduate School of Science, Osaka University. I would like to express my sincerest gratitude to Professor Akihito Hashidzume for his kindest guidance and assistance throughout this study. I am also greatly indebted to Associate Professor Yuri Kamon for her helpful advice.

I would like to express my deep gratitude to Professor Sadahito Aoshima, and Professor Yoshinori Takashima for their careful review and precious comments. I would like to express my gratitude to Professor Sadahito Aoshima again for their kind support on measurements of absolute weight-average molecular weights.

I would like to thank all the group members of Hashidzume laboratory for their kindest help.

I appreciate the Japan Science Society because this work was partly financial-supported by the Sasakawa Scientific Research Grant from the society.

Finally, I would like to extend my deep gratitude to my parents, husband, and friends for their loving considerations and warmest encouragements.

July 2020

XU LINLIN

Contents

Chapter 1

General Introduction

1-1. Copper(I)-Catalyzed Azide–Alkyne Cycloaddition in Polymerization

Huisgen cycloaddition (HC) is a 1,3-dipolar cycloaddition of alkynes and organic azides to form 1,2,3-triazole groups. HC is very classic and has widespread applications in the field of organic chemistry.[1,2,3] Upon heating, azides and alkynes can produce 1,2,3-triazole groups with high chemoselectivity without any additives and catalysts. However, thermal HC generally produces a mixture of 1,4- and 1,5-disubstituted 1,2,3-triazole regioisomers, as shown in Scheme 1-1. The poor regioselectivity limits the application of thermal HC as an effective conjugation strategy.

Scheme 1-1. Huisgen Cycloaddition (HC)

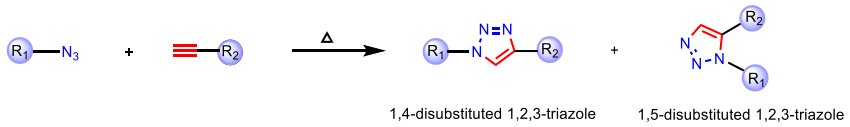

In 2001, Tornøe and Meldal[4] reported that HC of organic azides and alkynes is catalyzed by copper(I) compounds. In the same year, the concept of “click chemistry” was first introduced by Sharpless and coworkers.[5] In 2002, the highly

quantitative and regioselective ‘‘click’’ reaction, i.e., copper(I)-catalyzed azide–alkyne cycloaddition (CuAAC), has been developed independently by Meldal’s and Sharpless’ groups.[6,7] CuAAC gives only 1,4-disubstituted 1,2,3-triazoles, as shown in Scheme 1-2. Since CuAAC shows high tolerance to various functional groups, e.g., hydroxy, carboxy, and amino groups, CuAAC allows one to synthesize or modify target molecules carrying such functional groups. Based on its rapid, chemoselective, and quantitative nature, CuAAC has been thus utilized in a wide range of research fields, including sensor development,[8] bioconjugation,[9,10] and drug development,[11] as well as polymer science.[12-15]

Scheme 1-2. Copper(I)-Catalyzed Azide-Alkyne Cycloaddition (CuAAC).

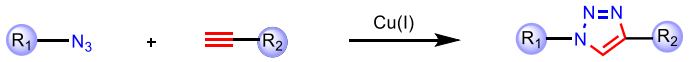

1,4-disubstituted 1,2,3-triazole

CuAAC has been widely utilized in polymer chemistry,[16] e.g., synthesis of sequence-defined polymers,[17] cyclic polymers,[18] and dendritic or hyperbranched polymers,[23] elongation of main chain,[19] side chain modification,[20] polymeric nanoparticles,[21] and cross-linking,[22] as shown in Figure 1-1. However, 1,2,3-triazole moieties are considered as “passive linkers” connecting polymer units in most of published works. The properties and applications of polymer composed

of 1,2,3-triazole moieties have been rarely addressed.

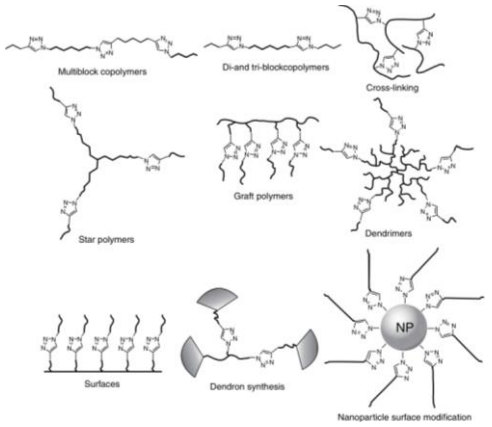

Figure 1-1. Variety of macromolecular architectures formed by CuAAC.[15] Reprinted with permission, Copyright 2009 by John Wiley & Sons, Inc.

1-2. 1,2,3-Triazole-Based Polymeric Functional Materials

1,2,3-Triazole is an aromatic five-membered ring consisting of two carbon and three nitrogen atoms with a large dipole,[24,25] which acts as an interaction site through hydrogen bonding, coordination bonding, dipole–dipole interaction, and π–π stacking.[26-28] On the basis of these unique properties of 1,2,3-triazole, the synthesis of functional materials possessing 1,2,3-triazole units has attracted considerable attention.[29-32] Furthermore, there is a lot of potential applications of 1,2,3-triazole-based functional polymeric materials synthesized by CuAAC, e.g.,

molecular recognition, tough network polymers, chemical sensing, drug discovery, and conducting materials.[33-38]

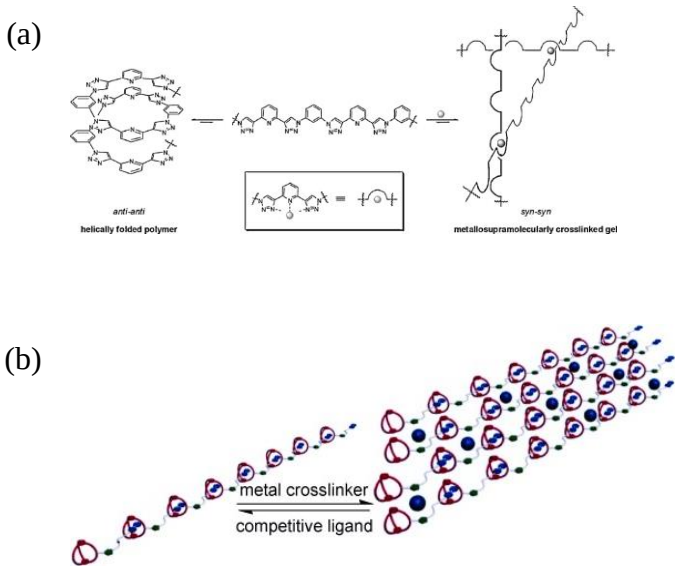

Figure 1-2. Supramolecularly cross-linked gels (a)[42] and cross-linked supramolecular polymers based on metal–1,2,3-triazole coordination (b).[43] Reprinted with permission, Copyright 2008 (a) and 2009 (b) WILEY–VCH.

Since 1,2,3-triazole coordinates with transition metals, 1,2,3-triazole-based ligands have been developed.[39-41] Recently, some groups utilized the coordination of 1,2,3-triazole and metals to form cross-linked supramolecular assemblies, as shown in Figure 1-2. In 2008, Hecht and coworkers[42] reported formation of supramolecularly cross-linked gel based on metal–1,2,3-triazole coordination

(Figure 1-2a). The 1,2,3-triazole moieties in polymer main chain can act as ligands for various transition metal ions, including Zn^{2+}, Fe^{2+}, and Eu^{3+}. Therefore, metal-containing gels can be prepared efficiently by addition of the desired metal ions. The formation of the bridging metal complexes is expected to offer a method for design of new magnetic (Fe) or emissive (Eu) materials. In 2009, Huang and coworkers[43] reported the formation of supramolecular polymer networks through palladium–ligand interaction based on the 1,2,3-triazole moieties (Figure 1-2b). Upon addition of $[PdCl_2(PhCN)_2]$, the 1,2,3-triazole moieties in linear polymers replaced the PhCN ligands of $[PdCl_2(PhCN)_2]$ to form a disubstituted palladium(II) complex, resulting in the formation of palladium-cross-linked supramolecular polymers formed from the linear supramolecular polymer. This study provides an efficient method to construct smart materials through the topological control of macromolecules based on 1,2,3-triazole–metal ion complexes.

Improvement of the polymer properties based on 1,2,3-triazole groups has attracted growing attention from scientists. For example, the intrinsically conducting polymers possessing 1,2,3-triazole moieties have been investigated by Coughlin and colleagues (Figure 1-3).[44] This study investigated the effect of the 1,2,3-triazole as the proton carrier on the conductivity of copolymers of 1,2,3-triazole-containing polyacrylates and poly(ethylene glycol)methyl ether acrylate (PEGMEA). Compared with benzimidazole polyacrylate, the more weakly basic

triazole containing polyacrylate showed a higher proton conductivity and a less pronounced temperature dependence of the conductivity. This unique behavior can be partly attributed to the higher pK_b of 1,2,3-triazole.

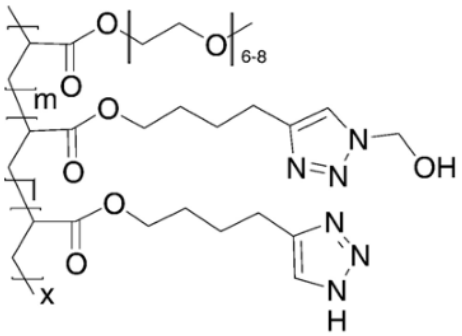

Figure 1-3. Conducting copolymers possessing 1,2,3-triazole-containing acrylates and PEGMEA.[44] Reprinted with permission, Copyright 2007 Published by Elsevier B.V.

Another representative research is 1,2,3-triazole polymers modified hydroxy-type chelating agents. In 2016, Reshmi et al.[45] utilized propargyloxy terminated polytetramethylene oxide (PTMP) and an azide-bearing polymer viz. glycidyl azide polymer (GAP) by CuAAC to construct PTMP-GAP triazole networks (Figure 1-4). The new propellants based on PTMP triazole networks showed superior processability and good mechanical properties, especially acted as

binders in solid rocket fuels, compared with traditional polyurethane-based chelating agents.

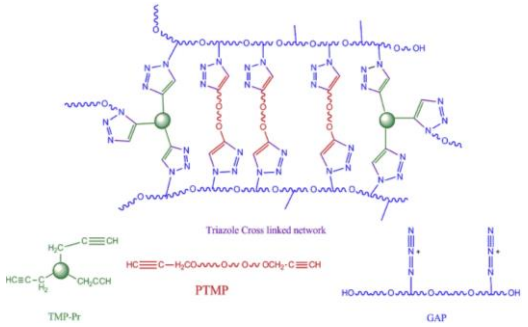

Figure 1-4. PTMP-GAP triazole networks: An effective binder for 'green' gas generator solid propellants.[45] Reprinted with permission, Copyright 2016 Elsevier Ltd.

The triazole nitrogenous heterocyclic can also act as a π-conjugated linker. Terao and coworkers[46] reported an AB-type insulated conjugated polymer by CuAAC reaction (Figure 1-5). In this work, CuAAC provides access to form conjugated polymers, and these conjugated polymers threaded through a series of permethylated cyclodextrin (PMCD) rings. Hence, the insulated conjugated polymers were obtained. Because of absence of aggregation of conjugated

polymers, this triazole-based functional polymers showed higher fluorescence quantum yields in solution than did the corresponding PMCD-free polymer.

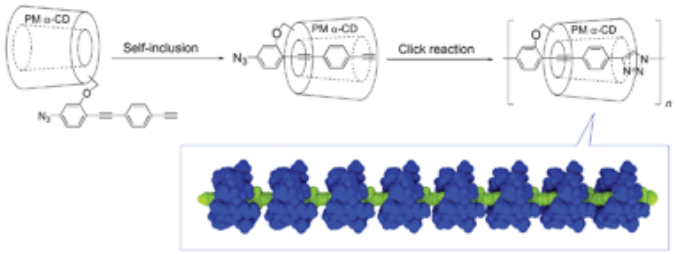

Figure 1-5. Insulated conjugated polymer wire by click polymerization.[46] Reprinted with permission, Copyright 2016 WILEY-VCH.

Significant advances on 1,2,3-triazole-based polymeric functional materials have been achieved and 1,2,3-triazole-based polymeric functional materials are promising in a variety of important applications. In the future, synthesis and characterization of 1,2,3-triazole-based polymeric functional materials are expected to be a hot topic.[47-49] However, to further explore the applications of 1,2,3-triazole polymers in more broader fields, including biochemistry, coordination chemistry, and supramolecular chemistry, scientists still need to pay more attention and efforts.

The application and function of polymer depend on their chemical structure. Most of the 1,2,3-triazole-based polymers reported so far possess 1,2,3-triazole units sparsely distributed, in the backbone, in which the triazole units are separated by longer spacers, or in the side chains.[50-54] One of the practical strategies to expand the applications of 1,2,3-triazole polymers is design novel polymers possessing dense 1,2,3-triazole moieties, which are thus promising as new functional materials.

1-3. Polymers Possessing Dense 1,2,3-Triazole Backbone

In 2013, Hashidzume et al.[55] constructed new polymers with the backbone composed of dense 1,2,3-triazole units by CuAAC of 3-azido-1-propyne (AP) and 3-azido-1-butyne (AB) bearing azide and alkyne functionalities linked via a carbon atom (Scheme 1-3). Because of their relevance to proteins, AP and AB oligomers are thus promising as functional polymers. However, the oligomers possessing dense 1,2,3-tirazole backbone were soluble only in strong acids, but insoluble in many organic solvents presumably because of strong inter/intramolecular dipole–dipole interactions.

Scheme 1-3. Oligomers Composed of Dense 1,2,3-Triazole Units[55]

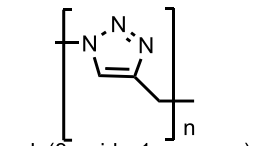

poly(3-azido-1-propyne)
PAP

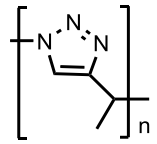

Poly(3-azido-1-butyne)
PAB

To improve the solubility of dense 1,2,3-triazole polymers in organic solvents for synthesis of high molecular weight polymers and investigate solution properties of the polymers, the authors developed the quaternization of the AP oligomer with methyl iodide[56] and diblock and triblock copolymers of dense 1,2,3-triazole and poly(ethyleneglycol) (PEG) blocks (Scheme 1-5).[57-59]

The EG*m*-*b*-AP*n* diblock copolymers are well soluble in many organic solvents, e.g., DMF, acetone, and dichloromethane. More interesting properties are EG*m*-*b*-AP*n* block copolymers form aggregates in water, e.g., spherical micelles and vesicles, depending on the ratio of block lengths, and undergo phase separation at higher temperatures because of cooperative dehydration of the PEG block.[58] The AP*n*-*b*-EG*m*-*b*-AP*n* triblock copolymers have shown excellent mechanical and self-healing properties because of strong interchain interactions between dense 1,2,3-triazole blocks and micro-phase-separated architecture.[59]

Scheme 1-5. AP*n*-*b*-EG*m*-*b*-AP*n* Triblock Copolymer[59]

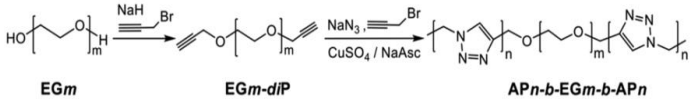

A more recent example in Hashidzume's group is the development of a new AP derivative possessing *t*-butyl (*t*-Bu) ester, i.e., *t*-butyl 4-azido-5-hexynoate (tBuAH). The monomer tBuAH was polymerized by CuAAC to yield a dense 1,2,3-triazole polymer soluble in organic solvents, e.g., polar and halogenated ones, indicating that the *t*-Bu ester side chains improved the solubility (Scheme 1-6).[60]

These researches on synthesis and characterization of dense 1,2,3-triazole polymers indicate that dense triazole-based systems exhibit distinct characteristics and polymers possessing the dense 1,2,3-triazole backbone are expected as unique functional materials, compared with the conventional 1,2,3-triazole polymers, in which 1,2,3-triazole units located loosely. However, there still exist many challenges; (1) How to introduce different functional group into 3-azido-1-propyne (AP), (2) how to construct sequence-defined dense 1,2,3-triazole polymers, and (3) how to characterize the function of dense 1,2,3-triazole polymers based on the unique property of 1,2,3-triazole.

Scheme 1-6. Dense 1,2,3-Triazole Poly(tBuAH) Soluble in Common Organic Solvents.[60]

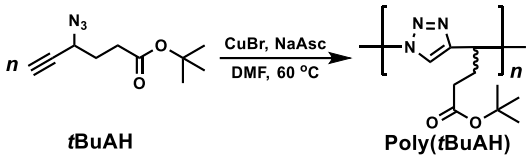

1-4. Scope of This Thesis

This work focuses on synthesis of new dense 1,2,3-triazole polymers which have different functional groups in the side chain, and investigation of their properties and application as new functional materials.

Chapter 2 describes that a new polyanion with a dense 1,2,3-triazole backbone, poly(4-azido-5-hexynoic acid) (poly(AH)), is synthesized by CuAAC polymerization of tBuAH followed by hydrolysis of the *t*-Bu ester groups. Turbidimetric and potentiometric titration data indicated that poly(AH) was well soluble in water under basic conditions and apparent pK_a = 5.4. Adsorption tests exhibit that sodium salt of poly(AH) (poly(AH)Na) adsorbs most preferably Fe^{3+} among the four metal ions examined, i.e., Cu^{2+}, Pb^{2+}, Li^{+}, and Fe^{3+}.

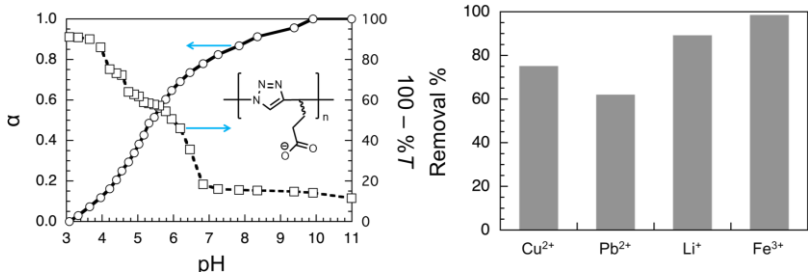

Figure 1-6. Turbidimetric and potentiometric titration for poly(AH) and adsorption behavior of poly(AH)Na for metal ions.

Chapter 3 describes an efficient synthetic strategy of 12-membered brominated cyclic compound, synthesis of cyclic dimer possessing azide and alkyne moieties and unique polycyclic polymer possessing dense 1,2,3-triazole backbone by CuAAC polymerization of the cyclic dimer. Because the polycyclic octamer is composed of the 12-membered macrocycle units, the optimized conformation of this polymer exhibits an interesting helix shape.

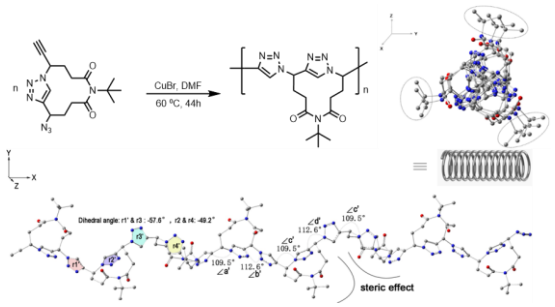

Figure 1-7. Polycyclic polymers possessing dense 1,2,3-triazole backbone and DFT-optimized conformation for the polycyclic octamer (16 monomer units).

Chapter 4 investigates the interaction of the polycyclic polymer with Pd^{2+} ions using a mixture of the polymer and $PdCl_2$ by ^1H NMR spectroscopy. The polymer–Pd complexes were dissociated by adding the strong ligand triphenylphoshine (PPh_3). Two-dimensional diffusion ordered spectroscopy (2D DOSY) indicated that the coordination of polycyclic polymer to Pd^{2+} made the polymer take a more compact conformation. ^1H NMR spectra were also measured at different temperatures. As the temperature was increased, the signals due to the complexed state became less significant.

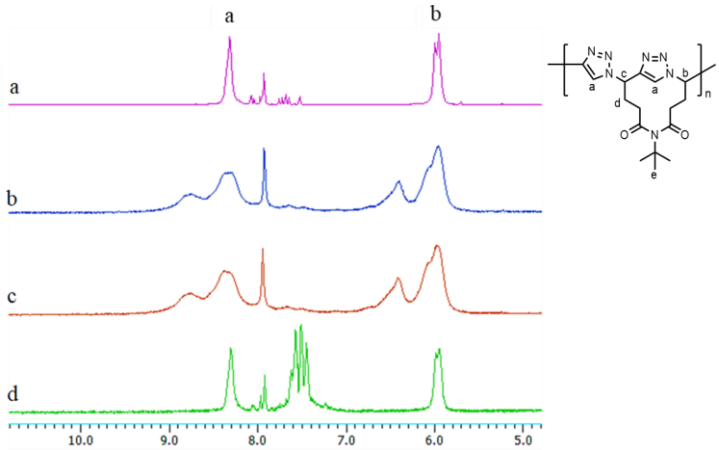

Figure 1-8. Interaction of the dense 1,2,3-triazole polycyclic polymer with $PdCl_2$.

The research content and conclusions of this work are summarized in Chapter 5.

References

1. Huisgen, R.; Szeimies, G.; Moebius, L. *Chem. Ber.* **1967**, *100*, 2494–2507.
2. Huisgen, R. in 1,3-Dipolar cycloaddition-introduction, survey, mechanism, ed. A. Padwa, New York, 1984.
3. Huisgen, R. *Pure Appl. Chem.* **1989**, *61*, 613.
4. Tornøe, C. W.; Meldal, M. Lebl, M.; Houghten, R. A. Eds., American Peptide Society and Kluwer Academic Publishers, San Diego 2001, pp. 263–264.
5. Kolb, H.C.; Finn, M.G.; Sharpless, K. B. *Angew. Chem. Int. Ed.* **2001**, *40*, 2004.
6. Tornøe, C. W.; Christensen, C.; Meldal, M. *J. Org. Chem*. **2002**, *67*, 3057–3064.
7. Rostovtsev, V. V.; Green, L. G.; Fokin, V. V.; Sharpless, K. B. *Angew. Chem. Int. Ed.* **2002**, *41*, 2596.
8. Zhang, X.; Zhang, Y. *Molecules* **2013**, *18*, 7145–7159.
9. Fuaad, A.A.H.; Azmi, F.; Skwarczynski, M.; Toth, I. *Molecules* **2013**, *18*, 13148–13174.
10. Tong, R.; Tang, L.; Ma, L.; Tu, C.; Baumgartner, R.; Cheng, J. *Chem. Soc. Rev*. **2014**, *43*, 6982–7012.
11. Thirumurugan, P.; Matosiuk, D.; Jozwiak, K. *Chem. Rev*. **2013**, *113*, 4905−4979.

12. Meldal, M. *Macromol. Rapid Commun*. **2008**, *29*, 1016–1051.
13. Li, H.; Aneja, R.; Chaiken, I. *Molecules* **2013**, *18*, 9797–9817.
14. Martens, S.; Holloway, J. O.; Prez, F. E. Du. *Macromol. Rapid Commun.* **2017**, *38*, 1700469.
15. Binder, W. H.; Zirbs, R. Encyclopedia of Polymer Science and Technology, Wiley, New York, 2009.
16. Johnson, J. A.; Finn, M. G.; Koberstein, J. T.; Turro, N. J. *Macromol. Rapid Commun*. **2008**, *29*, 1052–1072.
17. Barnes, J. C.; Ehrlich, D. J. C.; Gao, A. X.; Leibfarth, F. A.; Jiang, Y.; Zhou, E. Jamison, T. F.; Johnson, J. A. *Nat. Chem.* **2015**, *7*, 810–815.
18. Sugai, N.; Heguri, H.; Ohta, K.; Meng, Q.; Yamamoto, T.; Tezuka, Y. *J. Am. Chem. Soc*. **2010**, *132*, 14790–14802.
19. Pulst, M.; Samiullah, M. H.; Baumeister, U.; Prehm, M.; Balko, J.; Thurn-Albrecht, T.; Busse, K.; Golitsyn, Y.; Reichert, D.; Kressler, J. *Macromolecules* **2016**, *49*, 6609–6620.
20. Tejero, R.; Arbe, A.; Fernandez-Garcia, M.; Lopez, D. *Macromolecules* **2015**, *48*, 7180–7193.
21. O'Reilly, R. K.; Joralemon, M. J.; Hawker, C. J.; Wooley, K. L.; *New J. Chem.* **2007**, *31*, 718–724.
22. Martinez-Triana, Y. M.; Whelan, R.; Finn, M. G.; Diaz, D. D. *Macromol. Chem. Phys.* **2017**, *218*, 1600579.

23. Liang, L.; Astruc, D. *Coord. Chem. Rev.* **2011**, *255*, 2933–2945.

24. Dehaen, W.; Bakulev, V.A. Chemistry of 1,2,3-Triazoles; Springer: Cham, Switzerland, 2015.

25. Schulze, B.; Schubert, U.S. *Chem. Soc. Rev*. **2014**, *43*, 2522–2571.

26. Meudtner, R.M.; Hecht, S. *Macromol. Rapid Commun*. **2008**, *29*, 347–351.

27. Pourghaz, Y.; Dongare, P.; Thompson, D.W.; Zhao, Y. *Chem. Commun*. **2011**, *47*, 11014–11016.

28. Mishra, V.; Jung, S.-H.; Park, J.M.; Jeong, H.M.; Lee, H.-I. *Macromol. Rapid Commun*. **2014**, *35*, 442–446.

29. Gangaprasad, D.; Raj, J. P.; Kiranmye, T.; Sadik, S. S.; Elangovan, J. *RSC Adv*. **2015**, *5*, 63473–63477.

30. Monasterio, Z.; Irastorza, A.; Miranda, J. I.; Aizpurua, J. M. *Org. Lett*. **2016**, *18*, 2511–2514.

31. Chen, J.; Dongen, V. M. A.; Merzel, R. L.; Dougherty, C. A.; Kanduluru, B. G.; Orr, A. K.; Low, P. S.; Marsh, E. N. G.; Banaszak Holl, M. M. *Biomacromolecules* **2016**, *17*, 922–927.

32. Jalilian, F.; Yadollahi, B.; Tangestaninejad, S.; Rudbari, H. A. *RSC Adv*. **2016**, *6*, 13609–13613.

33. Wu, P.; Malkoch, M.; Hunt, J. N.; Vestberg, R.; Kaltgrad, E.; Finn, M. G.; Fokin, V. V.; Sharpless, K. B.; Hawker, C. J.; *Chem. Commun*. **2005**, 5775–5777.

34. Meudtner, R. M.; Hecht, S. *Macromol. Rapid Commun.* **2008**, *29*, 347-351.

35. Mishra, V.; Jung, S. H.; Park, J. M.; Jeong, H. M.; Lee, H. I. *Macromol. Rapid Commun.* **2014**, *35*, 442–446.

36. Sandmann, B.; Happ, B.; Kupfer, S.; Schacher, F. H.; Hager, M. D.; Schubert, U. S. Macromol. Rapid Commun. 2015, 36, 604−609.

37. Hou, X.; Ke, C.; Stoddart, J. F. *Chem. Soc. Rev*. **2016**, *45*, 3766–3780.

38. Shi, Y.; Cao, X.; Gao, H. *Nanoscale* **2016**, *8*, 4864–4881.

39. Li, Y.; Huffman, J. C.; Flood, A. H. *Chem. Commun*. **2007**, 2692–2694.

40. Badeche, S.; Daran, J. C.; Ruiz, J.; Astruc, D. *Inorg. Chem*. **2008**, 47, 4903–4908.

41. Wang, F.; Zhang, J. Q.; Ding, X.; Dong, S. Y.; Liu, M.; Zheng, B.; Li, S. G.; Wu, L.; Yu, Y. H.; Gibson, H. W.; Huang F. H. *Angew. Chem. Int. Ed*. **2010**, *49*, 1090–1094.

42. Meudtner, R. M.; Hecht, S. *Macromol. Rapid Commun.* **2008**, *29*, 347–351.

43. Yu, Y. H.; Gibson, H. W.; Huang F. H. *Angew. Chem. Int. Ed*. **2010**, *49*, 1090–1094.

44. Martwiset, S.; Woudenberg, R. C.; Granados-Focil, S.; Yavuzcetin, O.; Tuominen, M. T.; Coughlin, E. B. *Solid State Ionics* **2007**, *178*, 1398–1403.
45. Reshmi, S.; Hemanth, H.; Gayathri, S.; Reghunadhan Nair, C. P. *Polymer* **2016**, *92*, 201–209.
46. Terao, J.; Kimura, K.; Seki, S.; Fujihara, T.; Tsuji, Y. *Chem. Commun*. **2012**, *48*, 1577–1579.
47. Meng, Z.; Xiang, J.-F.; Chen, C.-F.; *J. Am. Chem. Soc*. **2016**, *138*, 5652–5658.
48. Mendecki, L.; Chen, X.; Callan, N.; Thompson, D. F.; Schazmann, B.; Granados-Focil S.; Radu, A. *Anal. Chem*. **2016**, *88*, 4311–4317.
49. Zarnegaryan, A.; Moghadam, M.; Tangestaninejad, S.; Mirkhani, V.; Mohammadpoor, B. I. *Polyhedron* **2016**, *115*, 61–66.
50. Hu, H. Y.; Dong, T. D.; Sui, Y. Q.; Li, N. W.; Ueda, M.; Wang, L. J.; Zhang, X. *J. Mater. Chem. A* **2018**, *6*, 3560–3570.
51. Pretzel, D.; Sandmann, B.; Hartlieb, M.; Vitz, J.; Holzer, S.; Fritz, N.; Moszner, N.; Schubert, U. S. *J. Polym. Sci. Part A: Poly. Chem.* **2015**, *53*, 1843–1847.
52. Sandmann, B.; Happ, B.; Kupfer, S.; Schacher, F. H.; Hager, M. D.; Schubert, U. S. *Macromol. Rapid Commun.* **2015**, *36*, 604−609.
53. Song, H. B.; Baranek, A.; Worrell, B. T.; Cook, W. D.; Bowman, C. N. *Adv. Funct. Mater.* **2018**, *1801095*.

54. Elloumi, A. K.; Miladi, I. A.; Serghei, A.; Taton, D.; Aissou, K.; Ben Romdhane, H.; Drockenmuller, E. *Macromolecules* **2018**, *51*, 5820–5830.
55. Hashidzume, A.; Nakamura, T.; Sato, T. *Polymer* **2013**, *54*, 3448–3451.
56. Nakano, S.; Hashidzume, A.; Sato, T. *Beilstein J. Org. Chem*. **2015**, *11*, 1037–1042.
57. Yang, Y.; Mori, A.; Hashidzume, A. *Polymers* **2019**, *11*, 1086.
58. Yang, Y.; Hashidzume, A. *Macromol. Chem. Phys*. **2019**, *220*, No. 1900317.
59. Yang, Y.; Kamon, Y.; Lynd, N. A.; Hashidzume, A. *Macromolecules* **2020**, *53*, 10323–10329.
60. Yamasaki, S.; Kamon, Y.; Xu, L.; Hashidzume, A. *Polymers* **2021**, *13*, 1627.

Chapter 2

Synthesis of a New Polyanion Possessing Dense 1,2,3-Triazole Backbone

2-1. Introduction

Polyanions are an important class of water soluble polymers showing various effects, e.g., thickening, gelling, dispersing, cohesive, adhesive, moisturizing, and metal ion scavenging effects. On the basis of the effects, polyanions are thus utilized in a wide range of industrial fields including detergents, cosmetics, pharmaceuticals, foods, paints, textiles, civil engineering, and construction.[1-6] There are a number of polyanions, which are categorized into natural, semi-synthetic, and synthetic polymers. Polyanions are composed of the polymer backbone, anionic residues, and linkers between the backbone and anionic residues. Polyanions are used in appropriate applications depending on their properties based on the chemical structure. Therefore, it is a great challenge to develop polyanions with novel structures to make their applications broader.

1,2,3-Triazole is an aromatic five-membered ring consisting of two carbon and three nitrogen atoms with a large dipole,[7,8] which acts as an interaction site through hydrogen bonding, coordination bonding, dipole–dipole interaction, and

π–π stacking.[8-14] 1,2,3-Triazoles are readily formed from azide and alkyne functionalities through 1,3-dipolar cycloaddition.[7,15-17] In particular, it is known that 1,4-disubstituted 1,2,3-triazoles are formed efficiently and selectively in the presence of copper(I) compounds.[18-20] This reaction is known as copper(I)-catalyzed azide–alkyne cycloaddition (CuAAC). Because of its tolerance, CuAAC has been used in a variety of fields as the most important reaction in click chemistry.[21,22] CuAAC has been also utilized for synthesis of polymers possessing 1,2,3-triazole units.[23-26] Hashidzume and coworkers[27-31] have been working on synthesis of polymers with the backbone composed of dense 1,2,3-triazole units by CuAAC polymerization of 3-azido-1-propyne (AP) and its derivatives. Unfortunately, AP polymer was insoluble in all the solvents examined presumably because of strong dipole–dipole interaction of dense 1,2,3-triazole units.

Recently, *t*-butyl 4-azido-5-hexynoate (tBuAH), which Yamasaki et al.[32] designed and synthesized, was polymerized by CuAAC to yield a dense 1,2,3-triazole polymer soluble in organic solvents, including polar and halogenated ones, indicating that the *t*-butyl (*t*-Bu) ester side chains improved the solubility. Since *t*-Bu ester is often used as a protecting group for carboxylic acid residue, a new polyanion, poly(4-azido-5-hexynoic acid) (poly(AH)), is obtained by hydrolysis of *t*-Bu ester, and the properties of poly(AH) are investigated preliminarily in this study.

2-2. Materials and Methods

Materials. Tetrahydrofuran (THF), copper(II) sulfate pentahydrate ($CuSO_4$•$5H_2O$), sodium (+)-ascorbate (NaAsc), ethylenediaminetetraacetic acid (EDTA), *N*,*N*-dimethylformamide (DMF), and dichloromethane (DCM) were purchased from FUJIFILM Wako Pure Chemical Co. (Osaka, Japan). Trifluoroacetic acid (TFA), copper(I) bromide (CuBr), sodium borohydride ($NaBH_4$), and lithium chloride (LiCl) were purchased from Nacalai Tesque Co., Ltd. (Kyoto, Japan). Lead(II) chloride ($PbCl_2$) and iron(III) nitrate ($Fe(NO_3)_3$•$9H_2O$) were purchased from Sigma-Aldrich (St. Louis, MO). Water was purified with a Millipore Milli-Q system. Other reagents were used as received.

Measurements. ^{1}H NMR spectra were measured on a JEOL JNM ECA400 spectrometer using tetramethylsilane (TMS) as an internal standard in $CDCl_3$ as a solvent at 25 °C. Pulse-field-gradient spin-echo (PGSE) NMR data were obtained on a JEOL JNM ECA500 spectrometer at 25 °C using deuterium oxide (D_2O) as a solvent. The bipolar pulse pair stimulated echo (BPPSTE) sequence was applied.[33-35] The strength of pulsed gradients (g) was increased from 0.3 to 90 gauss cm^{-1}. The time separation of pulsed field gradients (Δ) and their duration (δ) were 0.15 and 0.002 s, respectively. The sample was not spun and the airflow was disconnected. The shape of the gradient pulse was rectangular, and its strength was varied automatically during the course of the experiments. Two-dimensional

diffusion ordered spectroscopy (2D DOSY) data were obtained by inverse Laplace transformation using the SPLMOD method.[36,37] ^{1}H spin-lattice relaxation times (T_1) were determined using a conventional inversion recovery technique with a 180°–τ–90° pulse sequence.[38-40] Size exclusion chromatography (SEC) analysis was carried out at 25 °C on a TOSOH HLC-8320GPC system equipped with an RI detector and TOSOH TSK SuperAWM-H columns, using dimethyl sulfoxide (DMSO) containing lithium bromide (1.05 g L^{-1}) as the eluent at a flow rate of 0.4 mL min^{-1}. The molecular weights were calibrated with seven standard samples of poly(ethylene glycol) (PEG) and poly(ethylene oxide) (PEO) (Scientific Polymer Products, Inc. (Ontario, NY)). Sample solutions were filtrated with a DISMIC-13JP PTFE 0.50 μm filter just prior to injection. Absolute weight-average molecular weight (M_w) was performed on a system composed of a Viscotek VE 1122 pump, two TOSOH TSKgel GMH_{HR}-M columns connected in series, and a Viscotek TDA 305 triple detector, which monitored signals by refractive index, laser light scattering (λ = 670 nm, θ = 7° and 90°, where λ and θ denote the wavelength of incident light and scattering angle, respectively), and differential pressure viscometer, using THF as an eluent at 40 °C. The molecular weights were determined using the light scattering signals along with the values of specific refractive index increment determined on an Otsuka Electronics DRM-3000 differential refractometer. Sample solutions were filtrated with a DISMIC-13JP

PTFE 0.50 μm filter (ADVANTEC, (Tokyo, Japan)) just prior to injection. Fourier transform infrared (FTIR) spectra were recorded on a JASCO FT/IR-4600 spectrometer equipped with a JASCO ATR PRO ONE cell.

Preparation of t-Butyl 4-Azido-5-Hexynoate (tBuAH).[32] A typical procedure for preparation of poly(AH) is described below (Scheme 2-1).

t-Butyl 4-azido-5-hexynoate (tBuAH) monomer was synthesized using succinic anhydride as the starting material, the product was purified by column chromatography obtain colorless oil (1.6 g, 82%). ^{1}H NMR (400 MHz, $CDCl_3$) δ 4.21 (td, J = 7.0, 2.3 Hz, 1H), 2.59 (d, J = 2.3 Hz, 1H), 2.41 (t, J = 7.0 Hz, 2H), 2.02 – 1.95 (m, 2H), 1.45 (s, 9H).

Preparation of Poly(4-azido-5-hexynoic acid) (Poly(AH)). A typical procedure for preparation of poly(AH) is described below (Scheme 2-2).

CuBr (39 mg, 10% eq) and NaAsc (160 mg, 30% eq) were added to a solution of tBuAH (560 mg, 2.7 mmol) in DMF (0.2 mL) under a nitrogen atmosphere. The reaction mixture was warmed using an oil bath thermostated at 60 °C with stirring for 48 h. After the reaction mixture was cooled down to room temperature, ethyl acetate (20 mL) was added to the mixture. The organic layer was washed with 0.50 M EDTA (2 × 10 mL) and with water (100 mL). The organic phase was dried with Na_2SO_4. The polymer obtained was recovered by reprecipitation with hexane (60 mL). The polymer was dried at 40 °C under reduced pressure (360 mg,

64 %). ^{1}H NMR ($CDCl_3$, 400 MHz) δ (ppm): 7.94 (1H, 1,2,3-triazole CH), 5.99 (1H, CH), 2.57 (2H, CH_2), 2.17 (2H, CH_2), 1.41 (9H, t-C_4H_9).

The poly(tBuAH) sample (155 mg, 0.74 mmol monomer units) was dissolved in DCM (3.7 mL). TFA (3.7 mL) was added to the solution. The reaction mixture was stirred for 60 min. The reaction mixture was diluted with methanol (100 mL) and the solvent was removed under reduced pressure to obtain the product, poly(AH). Poly(AH) was recovered as colorless solid after drying at 60 °C under reduced pressure (112.6 mg, 99% yield). ^{1}H NMR (D_2O, 400 MHz) δ (ppm): 8.35 (1H, 1,2,3-triazole CH), 6.06 (1H, CH), 2.62 (2H, CH_2), 2.10 (2H, CH_2).

The poly(AH) sample was then neutralized with an equimolar amount of 0.10 M NaOH, and the poly(AH) neutralized (poly(AH)Na) was then recovered by drying under reduced pressure at 45 °C for 12 h.

Scheme 2-1. Synthetic Route of *t*-Butyl 4-Azido-5-Hexynoate (tBuAH)

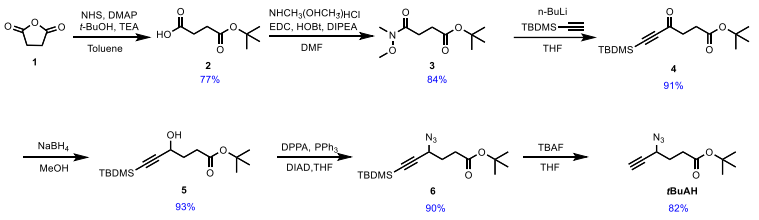

Turbidimetric and Potentiometric Titrations. A sample of poly(AH) not neutralized (68 μmol monomer units) was dissolved in 0.10 M NaOH (780 μL) and then diluted with water (5.4 mL). While the polymer solution was titrated with 0.10 M HCl from pH 10.9 using a microburet at 25 °C under a nitrogen atmosphere, turbidity and pH were monitored after establishing the equilibrated state, in which the pH reached a constant value after each step of titrant addition. Turbidities, reported as 100 – %*T*, were measured with a Brinkmann PC920 probe colorimeter equipped with a 1 cm path length fiber optics probe at 620 nm. Values of pH were measured with a Horiba F-23 pH meter equipped with a Horiba 9618S-10D glass electrode. The reference electrode was calibrated with buffer solutions of pH 4.01, 6.86, and 9.18 prior to pH measurements. The degrees of neutralization (α) were calculated from the amounts of the monomer unit and the added HCl.

***Adsorption Tests*.** Poly(AH)Na (11.5 mg, 65.7 μmol monomer units) was added to an aqueous solution of a salt (100 mg L^{-1} metal ion), i.e., $PbCl_2$, $CuSO_4 \cdot 5H_2O$, $(FeNO_3)_3 \cdot 9H_2O$, or LiCl, at pH = 7. The mixture was stirred at 35 °C for 12 h. After reaching equilibrium, 4 mL of the mixture solution was taken. The polymer–metal ion complexes were removed with a Pall MicrosepTM advanced centrifugal device 1K Omega (1 kDa cut off) by centrifugation at 1000 rpm for 15 min. The filtrate obtained (1.2 mL) was analyzed by a Perkin Elmer Optima 8300 ICP-Optical Emission Spectroscopy system to evaluate the

equilibrium concentration (c_e) of metal ion. The concentrations of metal ions in the equilibrated state were reported as average values of three measurements. The removal ratio ($r_{removal}$) and adsorption capacity (q_e) were calculated by

$$r_{removal} = \frac{100(c_i - c_e)}{c_i} \quad (1)$$

$$q_e = \frac{V(c_i - c_e)}{m} \quad (2)$$

where c_i is the initial ion concentration, m is the weight of poly(AH), and V is the volume of solution.

Scheme 2-2. Synthesis of Poly(AH) by CuAAC Polymerization of tBuAH Followed by Hydrolysis of the *t*-Bu ester

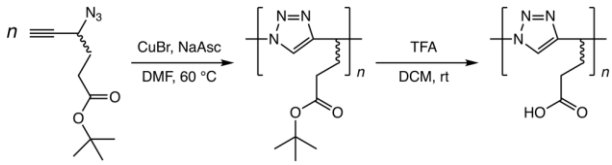

2-3. Results and Discussion

To prepare good solubility dense 1,2,3-triazole polymers poly(tBuAH), monomer tBuAH possessing a *t*-Bu ester moiety was synthesized according to the procedure developed in this group.[32]

According to the procedure reported previously, tBuAH was polymerized by CuAAC to yield poly(tBuAH) consisting of 1,4-disubstituted 1,2,3-triazole

residues.[32] These SEC (Figure 2-1), ^{1}H NMR (Figure 2-2a), and FTIR (Figure 2-3a) data are indicative of successful preparation of poly(tBuAH) samples. The basic characteristics of the copolymer samples were summarized in Table 2-1. The samples obtained in runs 2 ($M_w = 7.9 \times 10^3$) and 3 ($M_w = 8.8 \times 10^3$) were used as precursor polymers for synthsis of the poly(AH) samples in this study.

Table 2-1. Basic Characteristics of Poly(tBuAH) in This Study[a]

run	NaAsc (mol%)	CuBr (mol %)	NaAsc (eq)	Yield / %	M_w [c] / 10^3	M_w/M_n [c]	M_w [d] / 10^3
1[a]	1.1	10	0.3	65	10	1.5	—
2	1.1	10	0.3	68	7.9	1.5	26
3[b]	1.1	10	0.3	70	8.8	1.4	29
4	0.4	40	1.2	20	10	1.6	—
5	0.4	40	2.0	23	11	1.8	—
6	0.16	40	1.2	21	9.1	1.6	—

a. At 60 °C for 48 h unless otherwise indicated. *b*. At 60 °C for 168 h. *c*. Determined by SEC measurements at 25 °C using DMSO containing 1.05 g L^{-1} LiBr as eluent. Molecular weights were calibrated with PEG and PEO standard samples. *d*. Determined using light scattering signals obtained by SEC measurements at 30 °C using THF as eluent.

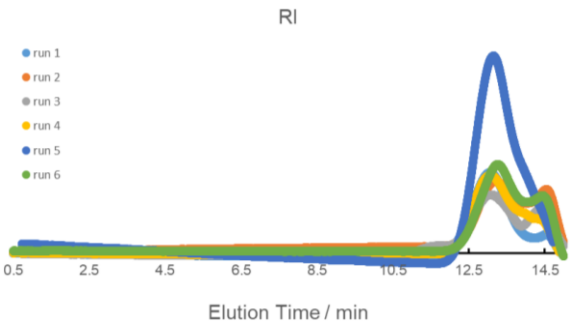

Figure 2-1. SEC data for poly(tBuAH) samples.

Poly(tBuAH) was soluble in many organic solvents, including polar and halogenated solvents, presumably because of the *t*-Bu ester moiety in the side chain. However, it was not dissolved in water. In this study, a new water-soluble polyanion, poly(AH), was synthesized by hydrolysis of the *t*-Bu ester moieties in poly(tBuAH). The poly(tBuAH) samples were dissolved in DCM, and the *t*-Bu ester groups were hydrolyzed with TFA to synthesize poly(AH) samples. Since poly(AH) is a weak polyanion possessing carboxylic acid moieties, the poly(AH) samples were neutralized with an equimolar amount of NaOH to dissolve in water, and then recovered as a salt-type polymer samples (poly(AH)Na) by drying under reduced pressure. Poly(AH) was characterized by ^{1}H NMR and FTIR. Figure 2-2 shows ^{1}H NMR spectra for poly(tBuAH) and poly(AH). As can be seen in Figure 2-2a, the spectrum of poly(tBuAH) in $CDCl_3$ contains signals ascribable to the proton in 1,4-disubstituted 1,2,3-triazole and the methine proton in the main chain

at ca. 7.9 and 6.0 ppm, respectively. The signals at ca. 2.6 and 2.2 ppm are assignable to the protons of two methylenes in side chain. The signal due to the *t*-Bu ester was observed at ca. 1.4 ppm. This ^{1}H NMR spectrum is thus indicative of successful preparation of poly(tBuAH) consisting of 1,4-disubstituted 1,2,3-triazole units. In the spectrum of poly(AH) in D_2O (Figure 2-2b), on the other hand, signals due to protons of the triazole, methine, and methylenes were observed, whereas the signal ascribable to the *t*-Bu ester was not observed. These observations indicate that poly(AH) was successfully obtained through quantitative hydrolysis of the *t*-Bu ester groups, as can be seen in Scheme 2-2.

Figure 2-3 displays FTIR spectra of poly(tBuAH) and poly(AH). Both the spectra indicate absorption bands ascribable to 1,2,3-triazole at ca. 1500, 1000, and 800 cm^{-1}. In the spectrum of poly(tBuAH), the signal attributed to the stretching vibration of the ester carbonyl was observed around 1720 cm^{-1}, whereas in the spectrum of poly(AH), a broad signal attributed to the carboxylic acid was observed around 1692 cm^{-1}. It should be noted here that the spectrum of poly(AH) contains a broad absorption band ascribable to the stretching vibration of O–H in the region of 2500 – 3500 cm^{-1} caused by intermolecular hydrogen bonding. These FTIR spectra also confirm that poly(AH) was successfully obtained by quantitative hydrolysis of the *t*-Bu ester groups in the side chain of poly(tBuAH) while the dense 1,2,3-triazole backbone was maintained.

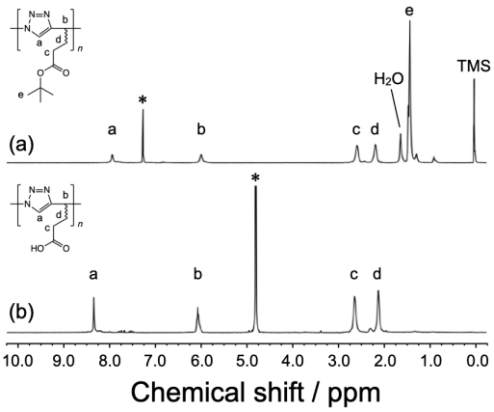

Figure 2-2. ^{1}H NMR spectrum for poly(tBuAH) ($CDCl_3$) (a) and poly(AH) (D_2O) (b).

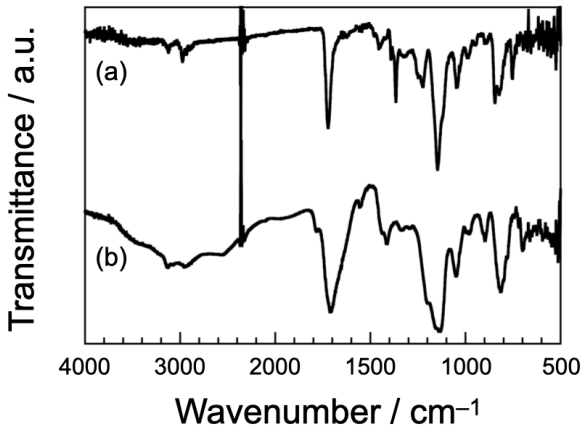

Figure 2-3. FTIR spectrum for poly(tBuAH) (a) and poly(AH) (b).

Turbidity and potentiometric titrations were carried out to study basic characteristics of poly(AH) as polyanion in aqueous media. The acid form of poly(AH) (10.4 mg, 68 μmol monomer units) and a small excess of NaOH (0.10 M, 780 μL) were dissolved in water (5.4 mL). Values of turbidity and pH were

recorded while hydrochloric acid (0.10 M) was added with a microburet to the polymer aqueous solution as a titrant with stirring under a nitrogen atmosphere. The dissociation degrees (α) were calculated using the mass of poly(AH) and the amount of HCl added, and the values of turbidity and α were plotted in Figure 2-4 against pH. As can be seen in Figure 2-4, the turbidity was almost 10% at pH > 7, whereas the turbidity increased with decreasing pH from 7 to 4, and then saturated at ca. 90% in the regime of pH < 4. On the other hand, α decreased with decreasing pH and reached 0 at ca. pH 3. The apparent pK_a at which α = 0.5 was estimated to be ca. 5.4, which is larger than that of polyacrylic acid (PAA) (pK_a = 4.5).[41] This observation indicates that poly(AH) is a weaker polyanion than PAA presumably because of the more hydrophobic backbone and linker of poly(AH).[42]

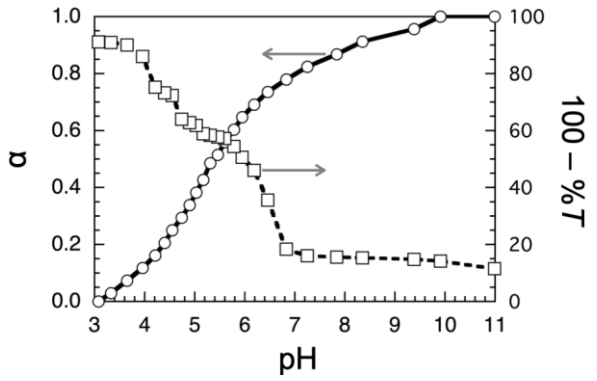

Figure 2-4. Turbidimetric and potentiometric titration data for an aqueous solution of poly(AH). The titration was performed by stepwise addition of 30 μL of 0.10 M HCl starting from pH 9.9.

The molecular sizes of poly(AH) chains in aqueous solution at pH 9.0 and 12.0 (i.e., pD 9.4 and 12.4, respectively) were estimated by PGSE NMR using D_2O containing 5 mM NaCl as a solvent. As can be seen in Figure 2-5, 2D DOSY data indicate that all the signals for poly(AH) were observed as unimodal distribution in the mutual diffu-sion coefficient (D) region of $(4.5 – 6.5) \times 10^{-11}$ and $(4 – 9) \times 10^{-11}$ m^2 s^{-1} at pH 9.0 and 12.0, respectively. (Here, the signals for methylene protons at ca. 2.2 ppm were not observed because the signals were very close to that for acetonitrile, the internal standard.) Using the signal attributed to the methine protons in main chain, the D values were evaluated to be 5.2×10^{-11} and 4.7×10^{-11} m^2 s^{-1} at pH 9.0 and 12.0, respectively. On the basis of these D values, the hydrodynamic radii were calculated to be ca. 3.4 and 3.7 nm at pH 9.0 and 12.0, respectively, using the Einstein–Stokes equation. These data indicate that poly(AH) takes a conformation independent of pH under basic conditions.

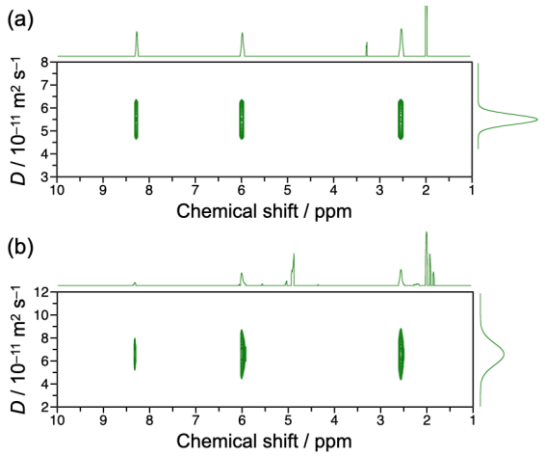

Figure 2-5. 2D DOSY data for poly(AH)Na in D_2O containing 5 mM NaCl at pH 9.0 (a) and 12.0 (b).

Poly(AH)Na possesses 1,2,3-triazole and carboxylate moieties in the monomer unit. Since 1,2,3-triazole and carboxylate moieties may act as relatively soft and hard ligands, respectively, poly(AH)Na may coordinate metal ions. Adsorption tests were thus performed using poly(AH)Na. Four salts, i.e., $CuSO_4•5H_2O$, $PbCl_2$, LiCl, and $Fe(NO_3)_3•9H_2O$, were added to an aqueous solution of poly(AH)Na, stirred for 12 h to reach adsorption equilibrium, and then the polymer was removed by centrifugal filtration. The equilibrium concentrations (c_e) of metal ions were determined by ICP measurements. Using the c_e value of metal ion, the removal ratio ($r_{removal}$) and the amount of metal ion adsorbed on 1.0 g of poly(AH)Na (adsorption capacity, q_e) were evaluated, as summarized in Table 2-2. The q_e values were 75.12 ± 0.02, 62.0 ± 0.2, 89.22 ± 0.02, and 98.57 ± 0.03

mg g^{-1} for the four metal ions used, i.e., Cu^{2+}, Pb^{2+}, Li^{+}, and Fe^{3+}, respectively (Figure 2-6). (Under the conditions in this study, the $r_{removal}$ values were almost the same as the q_e values; 75.10 ± 0.02, 62.0 ± 0.2, 89.20 ± 0.02, and 98.54 ± 0.03% for Cu^{2+}, Pb^{2+}, Li^{+}, and Fe^{3+}, respectively.) These observations indicate that poly(AH)Na can be used as an adsorbent for metal ions, especially Fe^{3+} ion.

Table 2-2. Removal Ratios ($r_{removal}$) and Adsorption Capacities (q_e) of poly(AH)Na for Metal Ions.

metal ion	c_i / mg L^{-1}	c_e / mg L^{-1}	$r_{removal}$ / %	q_e / mg g^{-1}
Cu^{2+}	100	24.90 ± 0.02	75.10 ± 0.02	75.12 ± 0.02
Pb^{2+}	100	38.0 ± 0.2	62.0 ± 0.2	62.0 ± 0.2
Li^{+}	100	10.80 ± 0.02	89.20 ± 0.02	89.22 ± 0.02
Fe^{3+}	100	1.46 ± 0.03	98.54 ± 0.03	98.57 ± 0.03

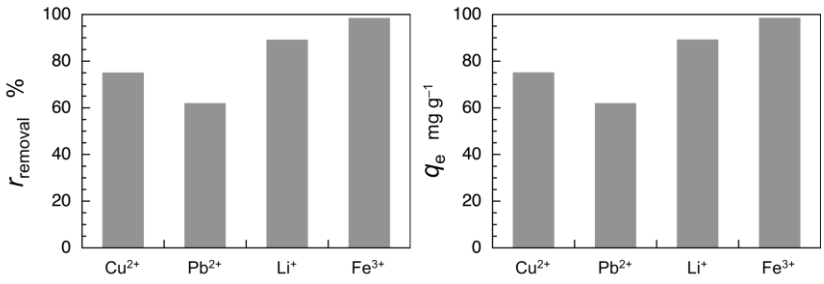

Figure 2-6. Removal ratio and adsorption capacity of poly(AH)Na for Cu^{2+}, Pb^{2+}, Li^{+}, and Fe^{3+}.

Since Fe^{3+} is a paramagnetic species, NMR relaxation may be significantly faster in the presence of Fe^{3+}. Figure 2-7 displays ^{1}H NMR spectra for poly(AH)Na in the presence of varying concentrations of $Fe(NO_3)_3$. The signals due to poly(AH)Na are only slightly broader at $[Fe^{3+}]$ = 0.1 mM. At $[Fe^{3+}]$ = 3.1 and 9.1 mM, on the other hand, the ^{1}H NMR spectra show markedly broader signals. It should be noted here that the signals due to the triazole and methine protons at ca. 8.2 and 6.0 ppm became weaker than did the signals due to the methylene protons at ca. 2.2. and 2.6 ppm. T_1 values of signals were measured and compared in ^{1}H NMR spectra in the presence and absence of 0.6 mM Fe^{3+} (Table 2-3). Figure 2-8 indicates the ratios of T_1 values for the ^{1}H NMR signals in the presence and absence of 0.6 mM Fe^{3+}. The ratio was 80.4% for the triazole proton at ca. 8.2 ppm, whereas those were 90.0 – 96.6% for the methine (6.0 ppm) and methylene protons (2.6 and 2.0 ppm). These observations indicate that Fe^{3+} ions are adsorbed more preferably onto the 1,2,3-triazole residues.[43,44]

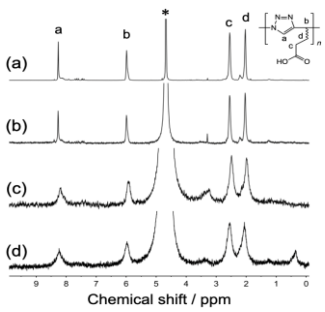

Figure 2-7. ^{1}H NMR spectrum for poly(AH)Na in the absence (a) and presence of 0.1 (b), 3.1 (c), and 9.1 mM of $Fe(NO_3)_3$ (D_2O) (d).

Table 2-3. ^{1}H NMR Chemical Shifts and T_1 Values for Poly(AH)Na in the Absence and Presence of 0.6 mM $Fe(NO_3)_3$

δ / ppm	$T_{1,pAH}$ [a] / s	$T_{1,pAHFe}$ [b] / s	$T_{1,pAHFe}$ / $T_{1,pAH}$
8.2	1.47	1.18	0.804
6.0	1.22	1.10	0.900
2.6	0.376	0.363	0.966
2.0	0.485	0.452	0.932

a. T_1 value for poly(AH)Na in the absence of $Fe(NO_3)_3$. *b*. T_1 value for poly(AH)Na in the presence of 0.6 mM $Fe(NO_3)_3$.

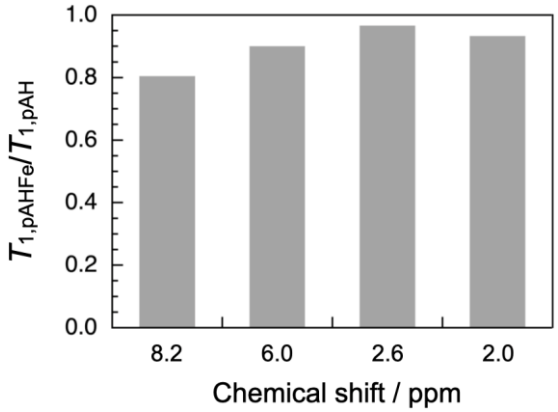

Figure 2-8. $T_{1,pAHFe}/T_{1,pAH}$ for ^{1}H NMR signals.

2-4. Conclusions

As a new polyanion with a dense 1,2,3-triazole backbone, poly(AH), was synthesized by CuAAC polymerization of tBuAH followed by hydrolysis of the *t*-Bu ester groups. The ^{1}H NMR and FTIR data confirmed the structure of

poly(AH). Turbidimetric and potentiometric titration date indicated that poly(AH) was well soluble at pH > 7, slightly soluble in the pH region of 7 – 4, and practically insoluble in the regime of pH < 4. The apparent pK_a at which $\alpha = 0.5$ was estimated to be ca. 5.4, which is larger than that of PAA (pK_a = 4.5), indicating that poly(AH) is a weaker polyanion than PAA presumably because of the more hydrophobic backbone and linker of poly(AH). On the basis of PGSE NMR data, the hydrodynamic radii of poly(AH)Na were estimated to be ca. 3.4 and 3.7 nm at pH 9.0 and 12.0, respectively, indicating that that poly(AH) takes a conformation independent of pH under basic conditions. Since 1,2,3-triazole and carboxylate moieties may act as relatively soft and hard ligands, respectively, adsorption tests were thus performed using poly(AH)Na. The amounts adsorbed were 75.12 ± 0.02, 62.0 ± 0.2, 89.22 ± 0.02, and 98.57 ± 0.03 mg g^{-1} for Cu^{2+}, Pb^{2+}, Li^{+}, and Fe^{3+}, respectively. These observations indicate that poly(AH)Na can be used as an adsorbent for metal ions, especially for Fe^{3+} ion. The ratio of T_1 values for the ^{1}H NMR signals in the presence and absence of 0.6 mM Fe^{3+} was calculated to be 80.4% for the triazole proton at ca. 8.2 ppm, whereas those were 90.0 – 96.6% for the methine (6.0 ppm) and methylene protons (2.6 and 2.0 ppm), indicating that Fe^{3+} ions are adsorbed more preferably onto the 1,2,3-triazole residues.

References

1. Tripathy, S.; Kumar, J.; Nalwa, H.S. *Handbook of polyelectrolytes and their applications*. American Scientific Publishers: Stevenson Ranch, CA, 2002.
2. Nussinovitch, A. *Water-soluble polymer applications in foods*. Blackwell Science Ltd: Oxford, UK, 2003.
3. Williams, P.A. *Handbook of industrial water soluble polymers*. Blackwell Publishing: Oxford, UK, 2007.
4. Rivas, B.L.; Pereira, E.; Maureira, A. *Polym. Int.* **2009**, *58*, 1093–1114.
5. Rivas, B.L.; Pereira, E.D.; Palencia, M.; Sánchez, J. *Prog. Polym. Sci.* **2011**, *36*, 294–322.
6. Kadajji, V.G.; Betageri, G.V. *Polymers* **2011**, *3*, 1972–2009.
7. Dehaen, W.; Bakulev, V.A. *Chemistry of 1,2,3-triazoles*. Springer: Cham, Switzerland, 2015.
8. Schulze, B.; Schubert, U.S. *Chem. Soc. Rev.* **2014**, *43*, 2522–2571.
9. Li, Y.; Huffman, J.C.; Flood, A.H. *Chem. Commun.* **2007**, 2692–2694.
10. Meudtner, R.M.; Hecht, S. *Macromol. Rapid Commun.* **2008**, *29*, 347–351.
11. Pourghaz, Y.; Dongare, P.; Thompson, D.W.; Zhao, Y. *Chem. Commun.* **2011**, *47*, 11014–11016.
12. Mishra, V.; Jung, S.-H.; Park, J.M.; Jeong, H.M.; Lee, H.-i. *Macromol. Rapid Commun.* **2014**, *35*, 442–446.
13. Wu, J.; Liu, W.; Han, H.; Sun, R.; Xie, M.; Liao, X. *Polym. Chem.* **2015**, *6*, 4801–4808.
14. Ghosh, K.; Panja, A.; Panja, S. *New J. Chem.* **2016**, *40*, 3476–3483.

15. Huisgen, R. *Angew. Chem., Int. Ed. Engl.* **1963**, *2*, 565–598.
16. Abboud, J.-L.M.; Foces-Foces, C.; Notario, R.; Trifonov, R.E.; Volovodenko, A.P.; Ostrovskii, V.A.; Alkorta, I.; Elguero, J. *Eur. J. Org. Chem.* **2001**, *2001*, 3013–3024.
17. Kolb, H.C.; Sharpless, K.B. *Drug Discovery Today* **2003**, *8*, 1128–1137.
18. Tornøe, C.W.; Christensen, C.; Meldal, M. *J. Org. Chem.* **2002**, *67*, 3057–3064.
19. Rostovtsev, V.V.; Green, L.G.; Fokin, V.V.; Sharpless, K.B. *Angew. Chem. Int. Ed.* **2002**, *41*, 2596–2599.
20. Fazio, F.; Bryan, M.C.; Blixt, O.; Paulson, J.C.; Wong, C.-H. *J. Am. Chem. Soc.* **2002**, *124*, 14397–14402.
21. Kolb, H.C.; Finn, M.G.; Sharpless, K.B. *Angew. Chem. Int. Ed.* **2001**, *40*, 2004–2021.
22. Lahann, J. *Click chemistry for biotechnology and materials science*. Wiley & Sons: Chichester, UK, 2009.
23. Qin, A.; Lam, J.W.Y.; Tang, B.Z. *Chem. Soc. Rev.* **2010**, *39*, 2522–2544.
24. Huang, D.; Liu, Y.; Qin, A.; Tang, B.Z. *Polym. Chem.* **2018**, *9*, 2853–2867.
25. Atanase, L.I.; Glaied, O.; Riess, G.. *Polymer* **2011**, *52*, 3074–3081.
26. Wei, Q.; Wang, J.; Shen, X.; Zhang, X.A.; Sun, J.Z.; Qin, A.; Tang, B.Z. *Sci. Rep.* **2013**, *3*, 1093.
27. Hashidzume, A.; Nakamura, T.; Sato, T. *Polymer* **2013**, *54*, 3448–3451.
28. Nakano, S.; Hashidzume, A.; Sato, T. *Beilstein J. Org. Chem.* **2015**, *11*, 1037–1042.

29. Yang, Y.; Mori, A.; Hashidzume, A. *Polymers* **2019**, *11*, 1086.
30. Yang, Y.; Hashidzume, A. *Macromol. Chem. Phys.* **2019**, *220*, 1900317.
31. Yang, Y.; Kamon, Y.; Lynd, N.A.; Hashidzume, A. *Macromolecules* **2020**, *53*, 10323–10329.
32. Yamasaki, S.; Kamon, Y.; Xu, L.; Hashidzume, A. *Polymers* **2021**, *13*, 1627.
33. Stejskal, E.O.; Tanner, J.E. *J. Chem. Phys.* **1965**, *42*, 288–292.
34. Tanner, J.E.; Stejskal, E.O. *J. Chem. Phys.* **1968**, *49*, 1768–1777.
35. Stilbs, P. *Prog. Nucl. Magn. Reson. Spectrosc.* **1987**, *19*, 1–45.
36. Morris, K.F.; Stilbs, P.; Johnson, C.S. *Anal. Chem.* **1994**, *66*, 211–215.
37. Huo, R.; Wehrens, R.; van Duynhoven, J.; Buydens, L.M.C. *Anal. Chim. Acta* **2003**, *490*, 231–251.
38. Erdmann, K.; Gutsze, A. *Colloid Polym. Sci.* **1987**, *265*, 667–673.
39. Raby, P.; Budd, P.M.; Heatley, F.; Price, C. *J. Polym. Sci., Part B: Polym. Phys.* **1991**, *29*, 451–456.
40. Brereton, M.G.; Ward, I.M.; Boden, N.; Wright, P. *Macromolecules* **1991**, *24*, 2068–2074.
41. Das, K.K.; Somasundaran, P. *Colloids Surf., A* **2001**, *182*, 25–33.
42. Hashidzume, A.; Morishima, Y.; Szczubiałka, K. In *Handbook of polyelectrolytes and their applications*, Tripathy, S.K.; Kumar, J.; Nalwa, H.S., Eds. American Scientific Publishers: Stevenson Ranch, CA, 2002; Vol. 2, pp 1-63.
43. Saravanan, N.; Yusuff, K.K.M. *Transition Met. Chem.* **1996**, *21*, 464–468.
44. You, X.; Wei, Z. *Inorg. Chim. Acta* **2014**, *423*, 332–339.

Chapter 3

Synthesis of a Polycyclic Polymer Possessing Dense 1,2,3-Triazole Backbone

3-1. Introduction

In the past decade, sequence control in synthetic polymers has been a hot topic in polymer synthesis.[1-7] There have been a number of examples on sequence-controlled polymers synthesized by chain and stepwise polymerizations so far.[8-29] The sequence-controlled polymers synthesized most easily are alternating copolymers composed of two comonomers. For example, copolymerization of two vinyl monomers that are not homopolymerized respectively form alternating copolymers. Using stepwise polymerization based on a reaction between functional groups A and B, alternating copolymers can be synthesized from a heterodimer of A-R^1-B and A-R^2-B monomers followed by polymerization of the heterodimer.

Recently, Yamasaki and coworkers[30] have designed and synthesized *t*-butyl 4-azido-5-hexynoate (tBuAH) as a monomer of CuAAC polymerization. tBuAH can be converted to a carboxylic acid, i.e., 4-azido-5-hexynoic acid (AH), by hydrolysis of the *t*-Bu ester, and thus various AH derivatives possessing a variety

of side chains can be synthesized by coupling of AH with alcohols and amines. Since a precursor of AH derivative carrying a *t*-butyldimethylsilyl (TBDMS) and hydroxy groups, i.e., a 6-*t*-butyldimethylsilyl-4-hydroxy-5-hexynoic acid derivative, can be selectively converted to reactive azide and alkyne forms by substitution of azide for the hydroxy group or by removal of the TBDMS protecting group, heterodimers can be synthesized and then polymerized to obtain alternating copolymers.

Aiming at synthesis of an alternating amphiphilic copolymer, a heterodimer of 4-azido-5-hexynic acid derivatives, tBuAH with *t*-Bu ester and 4-azido-*N*-*t*-butyl-5-hexynamide (tBuAHA) with *t*-Bu amide, was synthesized. CuAAC of the heterodimer will yield an alternating copolymer, of which *t*-Bu ester side chains are hydrolyzed under acidic conditions to form an alternating amphiphilic copolymer. During optimization of azidation, however, bromination of the heterodimer precursor possessing a hydroxyl group unexpectedly gave a brominated cyclic compound carrying a TBDMS-protected ethynyl group in a quantitative yield through cyclization and elimination of the *t*-butanol moiety (see Scheme 3-3). The formation of the cyclic compound has motivated the author to synthesis a unique polycyclic polymer. This chapter describes synthesis of a cyclic dimer possessing azide and alkyne moieties and its CuAAC polymerization to form a polycyclic polymer.

3-2. Materials and Methods

Materials. Tetrahydrofuran (THF), phosphorus tribromide (PBr_3), sodium azide (NaN_3), triphenylphosphine (PPh_3), sodium (+)-ascorbate (NaAsc), *N*,*N*-dimethylformamide (DMF), and dichloromethane (DCM) were purchased from FUJIFILM Wako Pure Chemical Co. (Osaka, Japan). Trifluoroacetic acid (TFA), acetic acid (AcOH), and copper(I) bromide (CuBr) were purchased from Nacalai Tesque Co., Ltd. (Kyoto, Japan). Tetrabutylammonium fluoride (TBAF), *t*-butylamine, diphenylphosphoryl azide (DPPA), and diisopropyl azodicarboxylate (DIAD) were purchased from Tokyo Chemical Industry Co. Ltd. (Tokyo, Japan). For thin layer chromatography (TLC) analysis throughout this work, Merck precoated TLC plates (silica gel 60 F 254) were used. The products were purified by column chromatography using silica gel 60 (Nacalai Tesque, spherical, neutrality). Other reagents were used as received.

t-Butyl 6-*t*-butyldimethylsily-4-hydroxy-l-5-hexynoate (**5**) was prepared according to the procedure of Yamasaki et al.[30]

Measurements. ^{1}H NMR and ^{13}C NMR measurements were carried out on a JEOL JNM ECA500 or ECS400 spectrometer at 25 °C using chloroform-*d* ($CDCl_3$) or dimethyl sulfoxided-d_6 (DMSO-d_6) as a solvent. Mass spectra (MS) were recorded on a Thermo Fisher Scientific Orbitrap XL using an electrospray ionization (ESI) source. Methanol was used as solvent. Internal calibration of ESI-

MS was carried out using the monoisotopic peaks of sodium adducted ion of diethylphthalate (*m*/*z* 314.1410), protonated ion of di-2-ethylhexylphthalate (*m*/*z* 391.2843), and sodium adducted ion of di-2-ethylhexylphthalate (*m*/*z* 413.2662). Size exclusion chromatography (SEC) analysis was carried out at 25 °C on a TOSOH HLC-8320GPC system equipped with an RI detector and TOSOH TSK SuperAWM-H columns, using dimethyl sulfoxide (DMSO) containing lithium bromide (1.05 g L^{-1}) as the eluent at a flow rate of 0.4 mL min^{-1}. The molecular weights were calibrated with seven standard samples of poly(ethylene glycol) (PEG) and poly(ethylene oxide) (PEO) (Scientific Polymer Products, Inc. (Ontario, NY)). Sample solutions were filtrated with a DISMIC-13JP PTFE 0.50 μm filter just prior to injection.

Synthesis of the monomers, and acyclic and cyclic dimers. The monomers, and acyclic and cyclic dimers were prepared according to Schemes 3-1– 3-3.

Scheme 3-1. Synthetic Route of *N*-(*t-Butyl*)-4-hydroxyhex-5-ynamide (8).

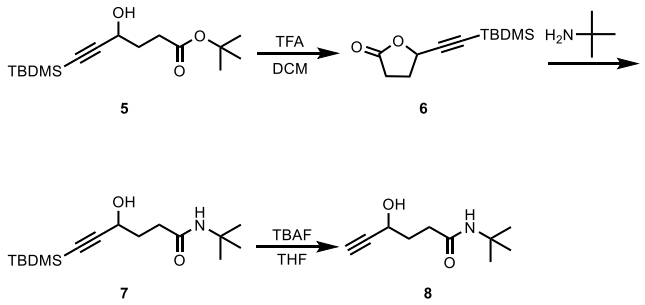

Scheme 3-2. Synthetic Route of *t*-Butyl 4-(4-(1-azido-4-(*t*-butylamino)-4-oxobutyl)-1H-1,2,3-triazol-1-yl)-5-hexynoate (12).

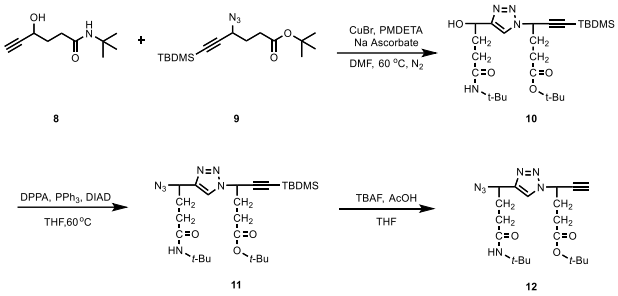

Scheme 3-3. Synthetic Route of (1^4*Z*,6*E*)-2-Azido-7-(*t*-butoxy)-10-ethynyl-1^{1}H-6-aza-1(1,4)-triazolacyclodecaphan-6-en-5-one (15).

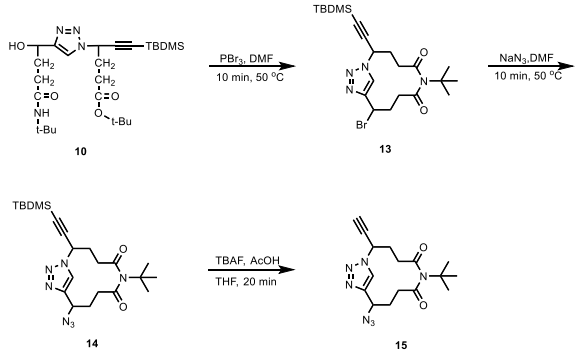

*Preparation of 5-((t-butyldimethylsilyl)ethynyl)oxolan-2-one (**6**).* To a solution of *t*-butyl 4-oxo-5-hexynoate **5** (2.5 g, 8.4 mmol) in DCM (26 mL) was added TFA (0.9 mL, 11.7 mmol) at 0 °C. The reaction mixture was allowed to warm to room temperature and stirred for 3 h. The resulting mixture was washed

with a saturated aqueous solution of $NaHCO_3$ (2 × 20 mL) and water (30 mL). The organic layer was dried over Na_2SO_4 and concentrated under reduced pressure to give 5-((*t*-butyldimethylsilyl)ethynyl)oxolan-2-one **6** (oil, 1.84 g, 98%). Compound **6** was used in the next step without further purification. ^{1}H NMR (400 MHz, $CDCl_3$) δ 5.14–5.11 (m, 1H), 2.68–2.54 (m, 1H), 2.53–2.49 (m, 2H), 2.32–2.29 (m, 1H), 0.93 (s, 9H), 0.12 (s, 6H). ^{13}C NMR (126 MHz, $CDCl_3$) δ 176.42, 101.77, 91.20, 69.44, 29.85, 27.74, 25.88, 16.28, –4.99. MS (ESI) *m*/*z*: calculated for $C_{12}H_{20}O_2SiNa$: 247.1125 $[M+Na]^+$, found: 247.1124 $[M+Na]^+$.

*Preparation of N-(t-butyl)-6-(t-butyldimethylsilyl)-4-hydroxy-5-hexynamide (**7**).* 5-((*t*-Butyldimethylsilyl)ethynyl)oxolan-2-one **6** (300 mg, 1.3 mmol) and *t*-butylamine (1.4 mL, 13 mmol) were placed in a 25 mL schlenk tube under a nitrogen atmosphere. The reaction mixture was heated at 150 °C and stirred for overnight. The tube was cooled to ambient temperature and opened. The reaction mixture was concentrated under reduced pressure to obtain *N*-(*t*-butyl)-6-(*t*-butyldimethylsilyl)-4-hydroxy-5-hexynamide **7** (oil, 384 mg, 99%). Compound **7** was used in the next step without further purification. ^{1}H NMR (400 MHz, $CDCl_3$) δ 5.37 (s, 1H), 4.48 (m, 1H), 2.54–2.48 (m, 1H), 2.33–2.26 (m, 1H), 2.04–1.97 (m, 2H), 1.34 (s, 9H), 0.93 (s, 9H), 0.10 (s, 6H). ^{13}C NMR (126 MHz, $CDCl_3$) δ 172.82, 107.30, 87.30, 61.93, 51.40, 33.37, 33.11, 28.78, 26.14, 16.49, –4.55. MS

(ESI) *m*/*z*: calculated for $C_{16}H_{31}NO_2SiNa$: 320.2016 $[M+Na]^+$, found: 320.2014 $[M+Na]^+$.

*Preparation of N-(t-butyl)-4-hydroxy-5-hexynamide (**8**)*. Compound **7** (228 mg, 0.76 mmol) was dissolved in THF (2 mL), followed by the slow addition of TBAF (1 M in THF, 1.5 mL) at 0 °C under a nitrogen atmosphere. The reaction mixture was stirred at room temperature for 2 h. The reaction mixture was concentrated under reduced pressure to obtain crude **8**. The product **8** was purified by column chromatography on silica gel (oil, 122 mg, 88%). ^{1}H NMR (400 MHz, $CDCl_3$) δ 5.40 (s, 1H), 4.54–4.49 (m, 1H), 4.21 (m, 1H), 2.57–2.53 (m, 1H), 2.45 (d, 1H), 2.35–2.32 (m, 1H), 2.29–2.28 (m, 1H), 2.08–2.05 (m, 1H), 1.34 (s, 9H). ^{13}C NMR (126 MHz, $CDCl_3$) δ 172.82, 107.30, 87.30, 61.93, 51.40, 33.37, 33.11, 28.78, 26.14, 16.49, –4.55. MS (ESI) *m*/*z*: calculated for $C_{16}H_{31}NO_2SiNa$: 206.1152 $[M+Na]^+$, found: 206.1151 $[M+Na]^+$.

*Preparation of t-butyl 4-(4-(4-(t-butylamino)-1-hydroxy-4-oxobutyl)-1H-1,2,3-triazol-1-yl)-6-(t-butyldimethylsilyl)-5-hexynoate (**10**).* Compounds **8** (160 mg, 0.87 mmol) and **9** (259 mg, 0.8 mmol) were dissolved in DMF (1.7 mL). CuBr (1.8 mg, 40), PMDETA (17 μL, 800μmol), and NaAsc (16 mg, 800 μmol) were added to the solution. The reaction mixture was heated at 60 °C for 48 h. The reaction mixture was concentrated under reduced pressure to obtain crude **10**. The dimer **10** was purified by column chromatography on silica gel (oil, 385 mg, 96%).

^{1}H NMR (400 MHz, $CDCl_3$) δ 7.76 (d, J = 2.0 Hz, 1H), 5.67 (d, J = 7.6 Hz, 1H), 5.52 (m, 1H), 4.97 (dt, J = 7.6, 2.0 Hz, 1H), 2.37–2.24 (m, 8H), 1.42 (s, 9H), 1.33 (s, 9H), 0.93 (s, 9H), 0.12 (s, 6H). ^{13}C NMR (126 MHz, $CDCl_3$) δ 173.39, 171.33, 152.00, 119.87, 100.23, 91.76, 81.10, 67.29, 60.50, 52.70, 51.59, 33.96, 32.75, 32.64, 32.59, 31.37, 31.30, 28.83, 28.18, 26.13, 16.58, –4.72. MS (ESI) *m*/*z*: calculated for $C_{26}H_{48}N_4O_4SiNa$: 529.3181 $[M+Na]^+$, found: 529.3177 $[M+Na]^+$.

*Preparation of t-butyl 4-(4-(1-azido-4-(t-butylamino)-4-oxobutyl)-1H-1,2,3-triazol-1-yl)-6-(t-butyldimethylsilyl)-5-hexynoate (**11**).* To a cooled solution (0 °C) of Ph_3P (21 mg, 80 μmol), DIAD (16 μL, 80 μmol) in THF (0. 2 mL) was added the compound **10** (20 mg, 40 μmol) under a nitrogen atmosphere. After 15 min, DPPA (17 μL, 80 μmol) was added and the reaction mixture was stirred for 16 min at room temperature and then the mixture was stirred for 20 min at 60 °C. The crude product was concentrated under reduced pressure. The product **11** was purified by TLC (oil, 7mg, 30%). ^{1}H NMR (400 MHz, $CDCl_3$) δ 7.75 (s, 1H), 5.56 (t, 1H), 5.48 (s, 1H), 4.73 (m, 1H), 2.42–2.25 (m, 8H), 1.44 (s, 9H), 1.35 (s, 9H), 0.95 (s, 9H), 0.15 (s, 6H). MS (ESI) *m*/*z*: calculated for $C_{26}H_{45}N_7O_3SiNa$: 554.3245 $[M+Na]^+$, found: 554.3228 $[M+Na]^+$.

*Preparation of t-butyl 4-(4-(1-azido-4-(tert-butylamino)-4-oxobutyl)-1H-1,2,3-triazol-1-yl)-5-hexynoate (**12**).* Compound **11** (4 mg) was dissolved in THF (0.2 mL), followed by the slow addition of AcOH (1 μL) and TBAF (14 μL) at –

20 °C under a nitrogen atmosphere. The reaction mixture was stirred at –20 °C for 15 min, and then the reaction was allowed to run at room temperature for 30 min. The resulting mixture was diluted with 10% citric acid (1 mL). The mixture was extracted with ethyl acetate (3 × 5 mL). The organic layer was washed with saturated aqueous solutions of $NaHCO_3$ (20 mL) and NaCl (20 mL), and dried with Na_2SO_4. The crude product was concentrated under reduced pressure. The product **12** was purified by TLC (oil, 2.4 mg, 77%). ^{1}H NMR (500 MHz, $CDCl_3$) δ 7.77 (s, 1H), 5.56 (m, 1H), 5.43 (s, 1H), 4.73 (m, 1H), 2.67 (m, 1H), 2.39–2.25 (m, 8H), 1.45 (s, 9H), 1.35 (s, 9H). ^{13}C NMR (126 MHz, $CDCl_3$) δ 171.13, 170.94, 146.75, 120.44, 81.29, 78.30, 77.41, 77.16, 76.91, 76.48, 57.12, 52.11, 51.44, 33.52, 32.21, 31.12, 30.30, 28.94, 28.19. MS (ESI) *m*/*z*: calculated for $C_{20}H_{31}N_7O_3Na$: 440.2381 $[M+Na]^+$, found: 440.2370 $[M+Na]^+$.

*Preparation of (1^{4}Z,6E)-2-bromo-7-(t-butoxy)-10-((t-butyldimethylsilyl) ethynyl)-1^{1}H-6-aza-1(1,4)-triazolacyclodecaphan-6-en-5-one (**13**).* To a solution of dimer **10** (340 mg, 870 μmol) in DMF (14 mL) was added PBr_3 (100 μL, 770 μmol) at room temperature under a nitrogen atmosphere. The reaction mixture was stirred at the 50 °C for 10 min. The flask was cooled to room temperature and the resulting mixture was diluted with cold saturated $NaHCO_3$ (20 mL). The mixture was extracted with ethyl acetate (3 × 100 mL). The organic layer was washed with water (4 × 100 mL), and dried by Na_2SO_4. The volatile fractions were removed

under reduced pressure to give compound **13** (oil, 309 mg, 93%). Compound **13** was used in the next step without further purification. ^{1}H NMR (500 MHz, $CDCl_3$) δ 7.81 (s, 1H), 5.55 (m, 1H), 5.27 (m, 1H), 2.67–2.41 (m, 4H), 2.40–2.31 (m, 4H), 1.44 (s, 9H), 0.95 (s, 9H), 0.16 (s, 6H). ^{13}C NMR (126 MHz, $CDCl_3$) δ 171.20, 171.19, 147.25, 121.61, 100.06, 99.71, 92.60, 81.27, 53.11, 41.38, 33.64, 32.51, 32.42, 31.31, 28.21, 26.11, 16.63, –4.73. MS (ESI) *m/z*: calculated for $C_{22}H_{35}BrN_4O_4SiNa$: 519.1584, 517.1584 $[M+Na]^+$, found: 519.1571, 517.1594 $[M+Na]^+$.

*Preparation of (1^{4}Z,6E)-2-azido-7-(t-butoxy)-10-((t-butyldimethylsilyl) ethynyl)-1^{1}H-6-aza-1(1,4)-triazolacyclodecaphan-6-en-5-one (**14**).* To a solution of compound **13** (309 mg, 810 μmol) in DMF (12 mL) was added NaN_3 (189 mg, 2.9 mmol) under a nitrogen atmosphere. The reaction mixture was stirred at 50 °C for 10 min. The resulting mixture was diluted with water (60 mL). The product was extracted with ethyl acetate (3 × 60 mL). The organic layer was washed with water (4 × 150 mL) and dried with Na_2SO_4. The volatile fractions were removed under reduced pressure to give compound **14** (oil, 268 mg, 94%). Compound **14** was used in the next step without further purification. ^{1}H NMR (500 MHz, $CDCl_3$) δ 7.80 (s, 1H), 5.58 (m, 1H), 4.83 (m, 1H), 2.58–2.30 (m, 8H), 1.44 (s, 9H), 0.95 (s, 9H), 0.16 (s, 6H). ^{13}C NMR (126 MHz, $CDCl_3$) δ 171.16, 144.86, 120.69, 99.72, 92.55, 81.23, 56.12, 53.10, 32.47, 31.25, 29.98, 28.18, 26.12, 16.59, 14.16, –4.76.

MS (ESI) *m*/*z*: calculated for $C_{22}H_{35}N_7O_2SiNa$: 480.2514 $[M+Na]^+$, found: 480.2496 $[M+Na]^+$.

*Preparation of (1⁴Z,6E)-2-azido-7-(t-butoxy)-10-ethynyl-1¹H-6-aza-1(1,4)-triazolacyclodecaphan-6-en-5-one (**15**).* AcOH (17.5 μL, 410 μmol) and a solution of TBAF in THF (1 M, 0.68 mL, 680 mmol) were added to a solution of compound **6** (268 mg, 590 mmol) in dry THF 26 mL at –18 °C under a nitrogen atmosphere. The reaction solution was stirred at –18 °C for 10 min. The reaction was then allowed to run at room temperature for 20 min. The reaction solution was diluted by ethyl acetate (100 mL) and washed with saturated NaCl (50 mL). The organic phase was dried with Na_2SO_4. After evaporation of the solvent, the product was purified by column chromatography to obtain colorless oil (188 mg, 93%). ^{1}H NMR (400 MHz, $CDCl_3$) δ 7.83 (d, J = 1.7 Hz, 1H), 5.61–5.57 (m, 1H), 4.83 (m, 1H), 2.69 (d, J = 1.7 Hz, 1H), 2.61–2.50 (m, 2H), 2.45–2.26 (m, 6H), 1.45 (s, 9H). ^{13}C NMR (126 MHz, $CDCl_3$) δ 171.05, 145.08, 120.84, 81.28, 76.63, 56.12, 52.20, 32.13, 31.04, 30.01, 28.14, 14.11. MS (ESI) *m*/*z*: calculated for $C_{16}H_{21}N_7O_2SiNa$: 366.1649 $[M+Na]^+$, found: 366.1649 $[M+Na]^+$.

Synthesis of an alternating copolymer by CuAAC of the acyclic dimer 12. A typical procedure for preparation of amphiphilic polymer is described below (Scheme 3-4).

CuBr (1.3 mg, 10% eq) and NaAsc (5.4 mg, 30% eq) were added to a solution

of compound **12** (38 mg, 91 μmol) in DMF (130 μL) under a nitrogen atmosphere. The reaction mixture was stirred at 60 °C for 48 h. After the reaction mixture was cooled down to room temperature, ethyl acetate (20 mL) was added to the mixture. The organic layer was washed with 0.50 M EDTA (2 mL) and water (50 mL). The organic phase was dried with Na_2SO_4. The polymer was recovered by reprecipitation with a mixed solvent of ethyl acetate and hexane (1/5, v/v). The polymer was dried at 40 °C under reduced pressure to obtain brown powder (28 mg, 74%).

Synthesis of polycyclic polymer by CuAAC of the cyclic dimer 15. A typical procedure for preparation of macrocyclic polymer is described below (Scheme 3-5).

CuBr (1.7 mg) were added to a solution of compound **15** (20 mg) in DMF (1.2 mL) under a nitrogen atmosphere. The reaction mixture was stirred at 60 °C for 48 h. After 48 h, diethyl ether (24 mL) was added to the reaction solution. The polymer was recovered by reprecipitation with a mixed solvent of DMF and diethyl ether (1/20, v/v). The polymer was dried at 40 °C under reduced pressure to obtain brown powder (17.8 mg, 89%).

Scheme 3-4. Synthesis of Alternating Copolymer by CuAAC

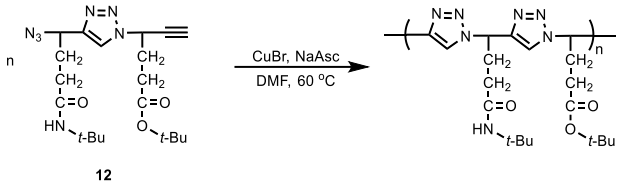

12

Scheme 3-5. Synthesis of Polycyclic Polymer by CuAAC

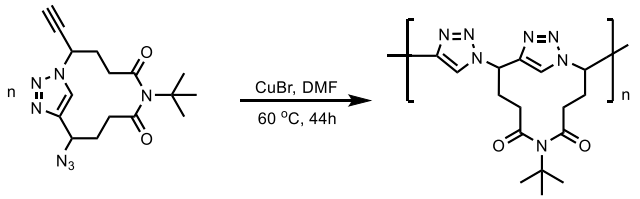

Density functional theory (DFT) calculation. DFT calculations were carried out for a polycyclic oligomer using the Gaussian 09 program[31] to estimate the stable conformation of oligomer. In all the calculations, DFT with B3LYP functional was used, and 6-31+G(d) basis sets were applied for the hydrogen, carbon, and nitrogen atoms. All the geometries were fully optimized.

3-3. Results and Discussion

Synthesis of monomers, and acyclic and cyclic dimers. In the present study, *t*-butyl 6-*t*-butyldimethylsilyl-4-hydroxy-5-hexynoate **5**,[30] a precursor of tBuAH, was used as the starting material. When **5** was treated with TFA in DCM, removal

of *t*-Bu group and cyclization occurred quantitatively to form a cyclic oxolane derivative **6**. The oxolane derivative **6** reacted with *t*-butylamine to give *N*-*t*-butyl-6-*t*-butyldimethylsilyl-4-hydroxy-5-hexynamide **7**. The TBDMS protecting group was deprotected with TBAF in THF to yield *N*-*t*-butyl-4-hydroxy-5-hexynamide **8** possessing a terminal ethynyl group. CuAAC of **8** with TBDMS-protected tBuAH **9** yielded a heterodimer precursor **10** of tBuAH and 4-azido-*N*-*t*-butyl-5-hexynamide (tBuAHA) using CuBr as a copper(I) catalyst in the presence of PMDETA and NaAsc. To synthesize alternating copolymers, the hydroxy group of the heterodimer **10** was azidated with DPPA to form the heterodimer precursor **11** in a lower yield (30%). The TBDMS protecting group of the acyclic heterodimer precursor was deprotected with TBAF in THF in the presence of acetic acid to obtain the acyclic heterodimer. This acyclic heterodimer **11** was characterized by ^{1}H NMR and ESI-MS. As can be seen in Figure 3-1, the ^{1}H NMR spectrum shows a signal ascribed to the 1,2,3-triazole and two methine protons at 7.75, 5.56, and 4.73 ppm, respectively. The spectrum also exhibits signals ascribed to the TBDMS protons at 0.95 and 0.15 ppm. There are signals ascribed to the amide, methylene, and *t*-Bu protons at proton at 5.48, 2.42–2.25, 1.44, and 1.35 ppm, respectively. The ratio of area intensities agrees well with the structure of compound **11**. The ESI-MS spectrum shows an intense signal assignable to the molecular ion $[C_{26}H_{45}N_7O_3Si + Na]^+$ at m/z = 554.3228, as shown in Figure 3-2.

These observations indicate that an azide group was successfully introduced into **11**.

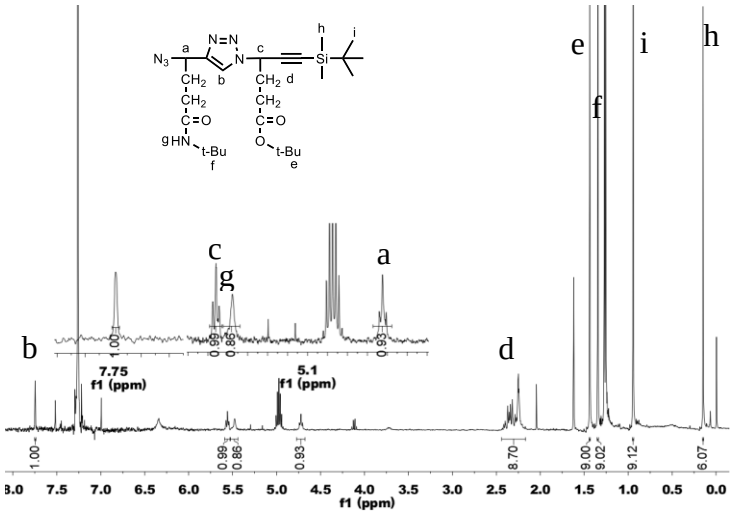

Figure 3-1. ^{1}H NMR spectrum of compound **11** ($CDCl_3$, 400 MHz).

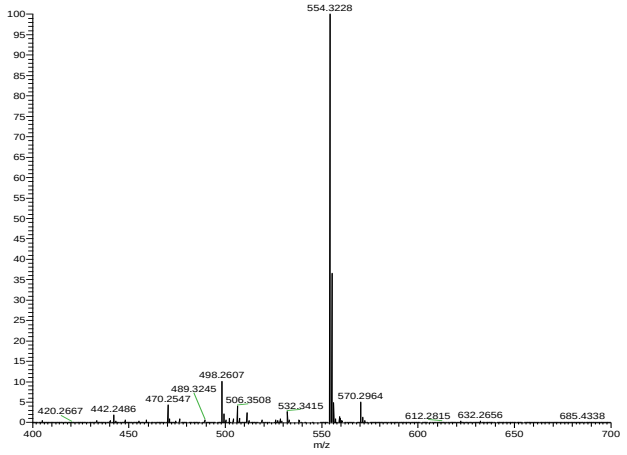

Figure 3-2. ESI-MS spectrum of compound **11**.

Since azidation of the corresponding bromide with sodium azide may be useful to improve the yield of compound **11**, compound **10** was treated with PBr_3 to form the corresponding bromide. Unexpectedly, however, a product **13** different from the bromide was obtained quantitatively. The structure of compound **13** was characterized by ESI-MS, ^{1}H NMR, and ^{13}C NMR spectra. As can be seen in Figure 3-3, the ESI-MS chart indicates signals at *m*/*z* = 517.1594 and 519.1571 that are consistent with the isotopic pattern of compounds possessing a bromine atom. These signals are ascribable to the sodium adduct ion of $C_{22}H_{35}BrN_4O_2Si$ molecule. Since the molecular formula of corresponding bromide is $C_{26}H_{45}BrN_4O_3Si$, the product **13** should be yielded after elimination of $C_4H_{10}O$, i.e., a *t*-butanol moiety, by treatment with PBr_3. Figure 3-4 displays the ^{1}H NMR spectrum for compound **13**. This ^{1}H NMR spectrum contains signals due to the TBDMS protecting group at 0.96 and 0.16 ppm. There are signals ascribable to the triazole and two methine protons at 7.81, 5.55, and 5.27 ppm, respectively. Signals assignable to protons of four methylenes were also observed in the region of 2.67 – 2.30 ppm. It is noteworthy that the ^{1}H NMR spectrum exhibits only a signal due to *t*-Bu group at ca. 1.5 ppm, supporting the elimination of a *t*-butanol moiety. These data as well as ^{13}C NMR (Figure 3-5) have indicated the compound **13** is a macrocycle, as shown in Scheme 3-3. Scheme 3-6 indicates a proposed mechanism for the formation of compound **13**. After the hydroxy group of

compound **10** is brominated with PBr_3, the *t*-Bu ester is converted to acyl bromide by excess PBr_3. The carbonyl carbon of the acyl bromide undergoes nucleophilic attack of the lone pair on the nitrogen of the *t*-Bu amide, resulting in ring closure with HBr elimination and shift of the *t*-Bu group to form compound **13**.

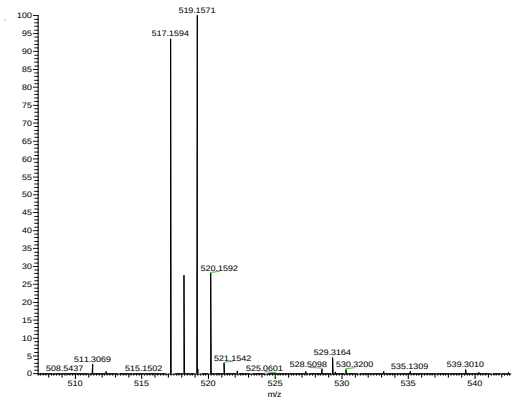

Figure 3-3. ESI-MS spectrum of compound **13**.

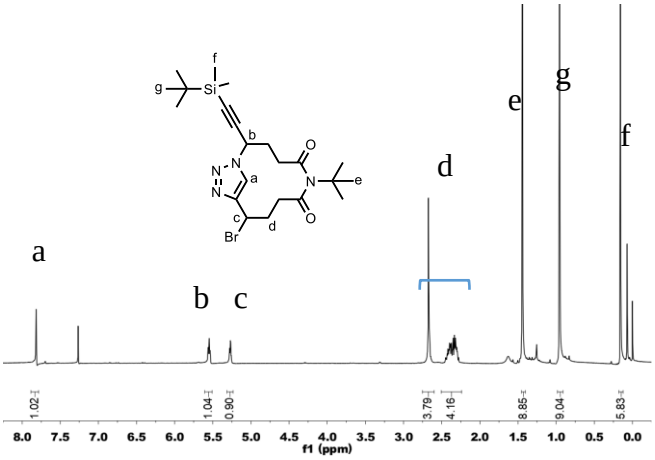

Figure 3-4. ^1H NMR spectrum of compound **13** ($CDCl_3$, 500 MHz).

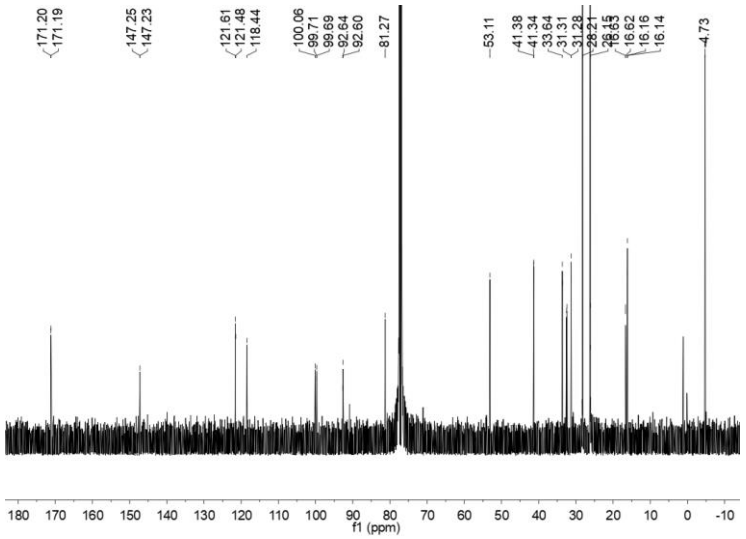

Figure 3-5. ^{13}C NMR spectrum of compound **13** ($CDCl_3$, 126 MHz).

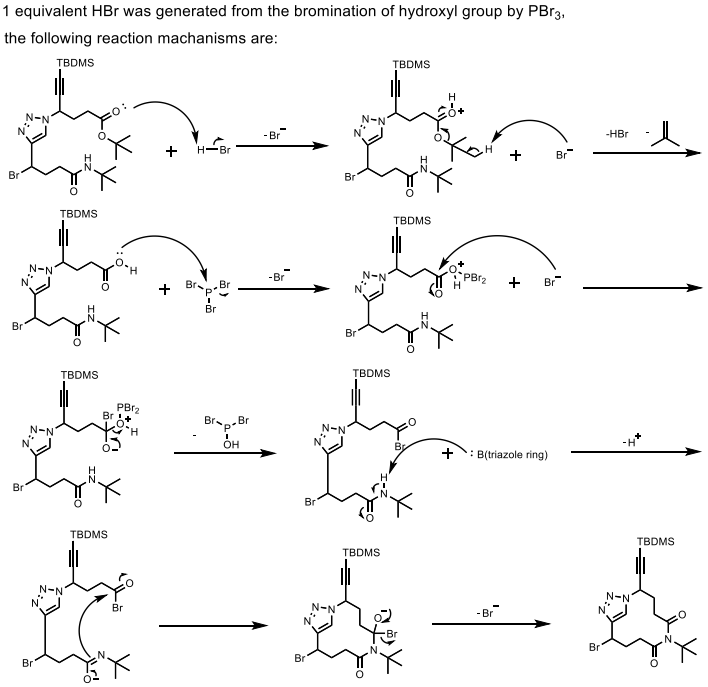

Scheme 3-6. A Proposed Mechanism for the Formation of Compound 13.

Compound **13**, which was formed unexpectedly, can be derived a cyclic monomer **15** of CuAAC after azidation of the bromo group and deprotection of TBDMS protecting group. It should be noted here that the polymer of **15** is polycyclic, i.e., a unique structure. Thus, a cyclic dimer **15**, was synthesized by azidation of compound **13** with sodium azide in DMF followed by deprotection of the TBDMS protecting group using TBAF in THF in the presence of acetic acid. Compound **15** was identified using ^{1}H NMR, ^{13}C NMR, ESI-MS, HSQC, HMBC, and NOESY. As shown in Figure 3-6, the ^{1}H NMR spectrum contains signals ascribed to the triazole and two methine protons at 7.83, 4.83, and 5.60 ppm, respectively. There are signals ascribable to the methylene and *t*-Bu protons at 2.57 – 2.31 and 1.45 ppm, respectively. A signal due to the ethynyl proton was observed at 2.70 ppm. The ^{13}C NMR spectrum also supported the formation of compound **15** (Figure 3-7). The ESI-MS spectrum shows an intense signal assignable to a molecular ion $[C_{16}H_{21}N_7O_2Si + Na]^+$ at m/z =366.1647, as shown in Figure 3-8.

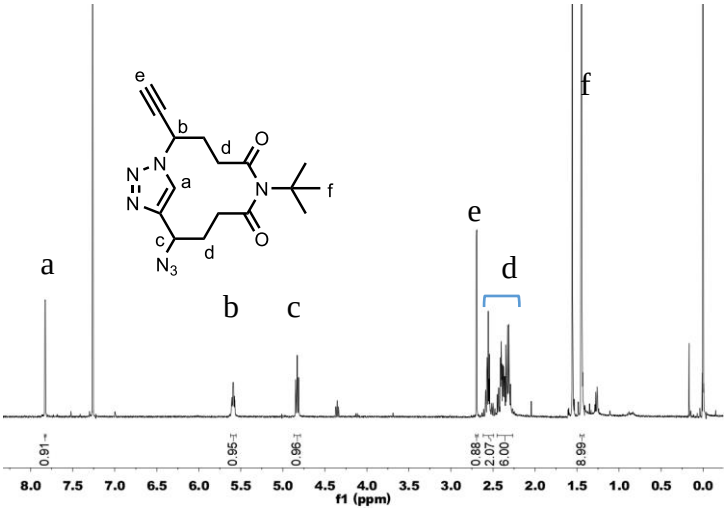

Figure 3-6. ^{1}H NMR spectrum of compound **15** ($CDCl_3$, 400 MHz).

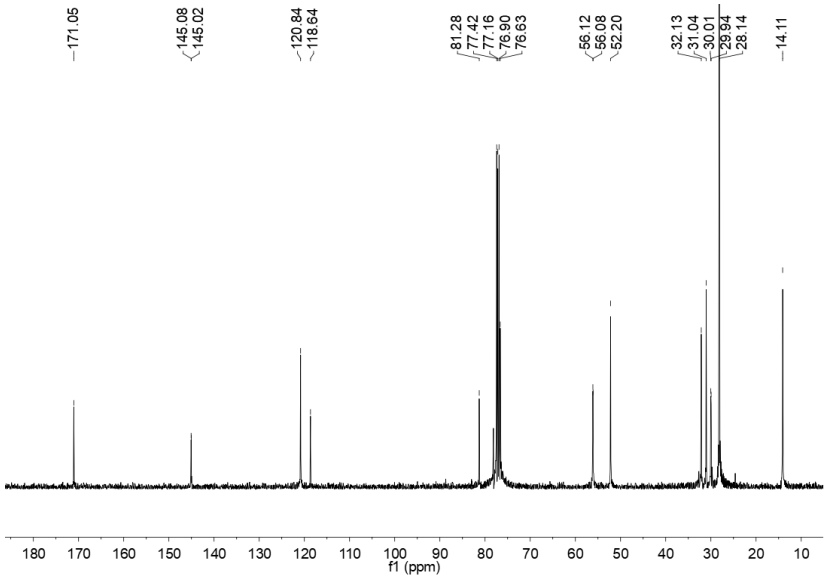

Figure 3-7. ^{13}C NMR spectrum of compound **15** ($CDCl_3$, 126 MHz).

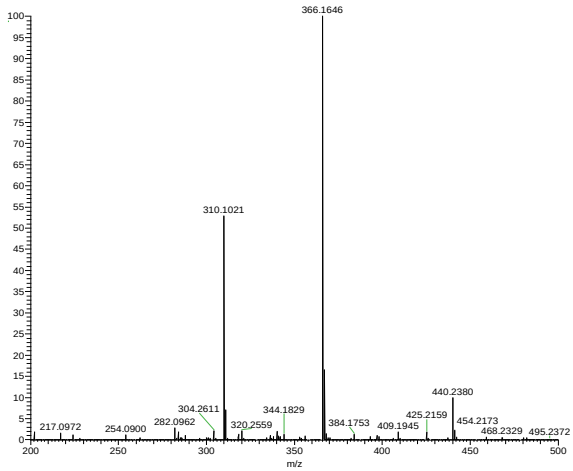

Figure 3-8. ESI-MS spectrum of compound **15**.

CuAAC polymerization of acyclic and cyclic dimers. According to Scheme 3-4, the acyclic heterodimer **12** possessing *t*-Bu amide and *t*-Bu ester side chain was polymerized by CuAAC in DMF using CuBr in the presence of NaAsc to obtain an alternating copolymer consisting of 1,4-disubstituted 1,2,3-triazole residues in a higher yield (74%, run 1 in Table 1). The polymer obtained was characterized by ^{1}H NMR and SEC. Figure 3-9 indicates that the ^{1}H NMR spectrum for the alternating copolymer contains signals assignable to the 1,2,3-triazole, amide, and methine protons at 8.36, 7.33, and 5.96 ppm, respectively. There are signals ascribable to the protons the *t*-Bu ester at ca. 1.33 and 1.18 ppm. The signals at ca. 2.6 – 2.1 ppm are assigned to the protons of four methylenes. This ^{1}H NMR spectrum indicates that an alternating copolymer of *t*-Bu ester and *t*-Bu amide side chains was successfully synthesized. The SEC chart for the

alternating copolymer indicated multimodal signals in the elution time range of 12 – 14 min (Figure 3-10). Using the SEC chart, the M_w for alternating copolymer was determined to be 1.1×10^4. These ^{1}H NMR and SEC data are indicative of successful preparation of an alternating copolymer possessing the dense 1,2,3-triazole backbone.

Table 3-1. Conditions and Results of CuAAC Polymerization of the Acyclic 12 and Cyclic Dimers 15

run	monomer	CuBr / mol%	conc. / M	M_w [a] / 10^3	M_w/M_n [a]	time / h	yield / %
1[b]	**12**	10	0.7	11	1.3	48	74
2[b]	**15**	10	1.1	4.7	1.4	48	53
3[c]	**15**	10	1.1	1.0	1.4	48	87
4	**15**	20	0.4	15	2.3	21	72
5	**15**	20	0.11	15	2.1	44	89
6	**15**	20	0.05	20	2.5	44	90

a. Determined by SEC measurements at 25 °C using DMSO containing 1.05 g L^{-1} LiBr as eluent. Molecular weights were calibrated with PEG and PEO standard samples. *b.* In the presence of NaAsc (30 mol%). *c*. In the presence of PMDTA (20 mol%) and NaAsc (30 mol%).

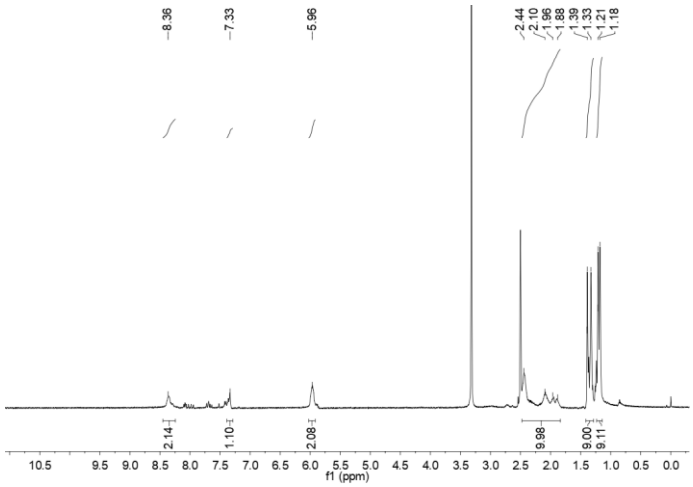

Figure 3-9. ^{1}H NMR spectra for alternating copolymer (DMSO-d_6, 400 MHz).

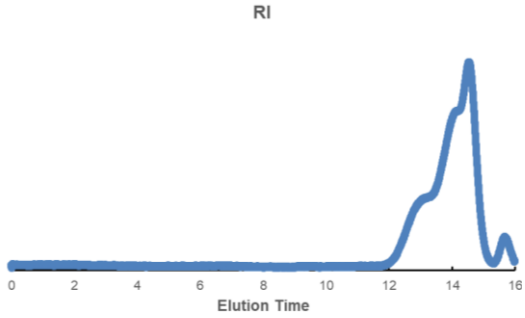

Figure 3-10. SEC trace for alternating copolymer (run 1 in Table 3-1).

Preparation of polycyclic polymer. To obtain polycyclic polymers possessing the dense 1,2,3-triazole backbone, the cyclic dimer **15** was polymerized by CuAAC using CuBr in DMF at 60 °C. The conditions and results are summarized in Table 3-1. In runs 1 and 2, NaAsc and PDMTA/NaAsc were

added as additives, respectively. It should be noted here that the M_w values for runs 4 – 6 were larger than those for runs 2 and 3 (Figure 3-11), indicating that a higher concentration of CuBr (20 mol%) is useful to obtain polycyclic polymers of higher M_w. The polymer structure was characterized by ^{1}H NMR. As can be seen in Figure 3-12, the ^{1}H NMR spectra of the polycyclic polymer contain signals assignable to the 1,2,3-triazole and methine protons at 8.4 and 6.04 ppm, respectively. A signal due to the dangling *t*-butoxy group was observed at ca. 1.3 ppm. The signals in the region of 2.6 – 2.1 ppm were assignable to the protons of methylenes in the macrocycle. These ^{1}H NMR spectra indicate that polycyclic polymers consisting of 1,4-disubstituted 1,2,3-triazole units was successfully synthesized.

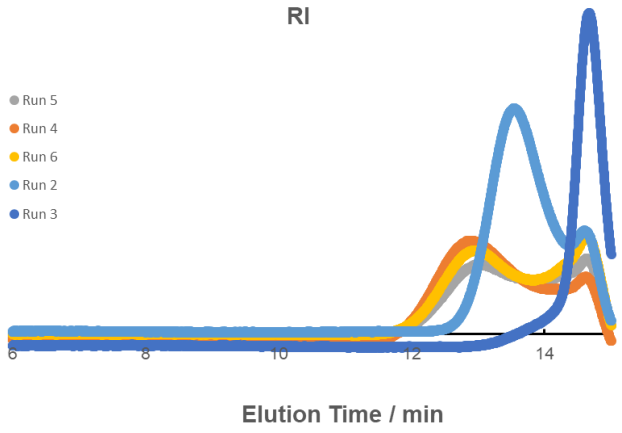

Figure 3-11. SEC charts for the polycyclic polymer samples (runs 2 – 6 in Table 3-1).

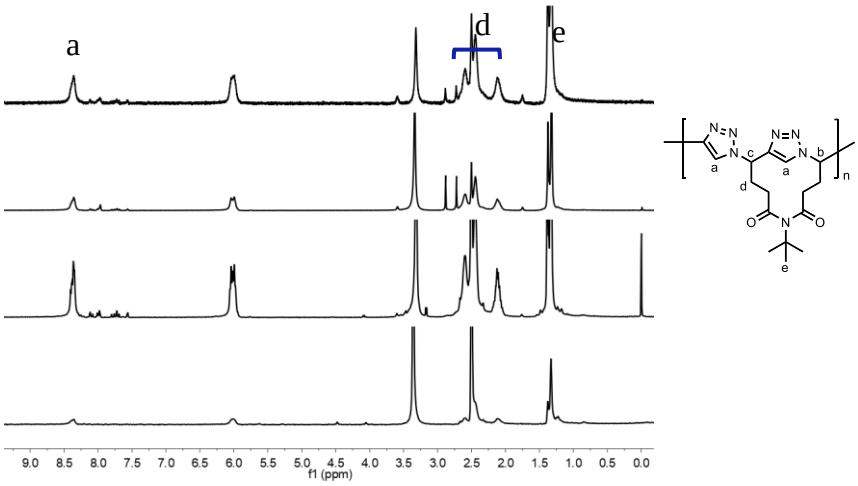

Figure 3-12. [1]H NMR spectra for the polycyclic polymer samples (runs 2 – 6 in Table 3-1) (DMSO-d_6, 500 MHz).

DFT consideration on stable conformation of the polycyclic polymer. In the previous work, the DFT calculation for diblock copolymers PEG and dense 1,2,3-triazole blocks has indicated that dense 1,2,3-triazole blocks, in which 1,2,3-triazole units linked through a methylene carbon, take elongated conformations.[32] The optimized conformation of polycyclic octamer (16 monomer units) was obtained by DFT calculation on the PM3 level using the Gaussian 09 program, as can be seen in Figure 3-13. This figure demonstrates that the polycyclic octamer takes a helix conformation. This may be because the polycyclic octamer is composed of the 12-membered macrocycle units that have ring‐ring repulsion

effect between the close macro-cycles based on the famous Pauling-repulsion theory, and 1,2,3-triazole linkers, which somehow fix the connecting angle.

(a)

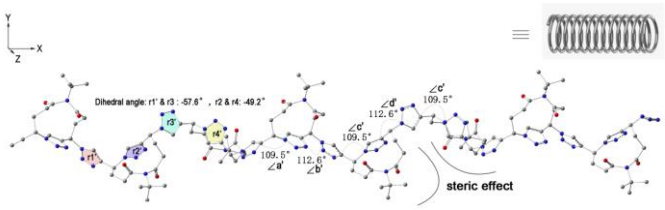

(b)

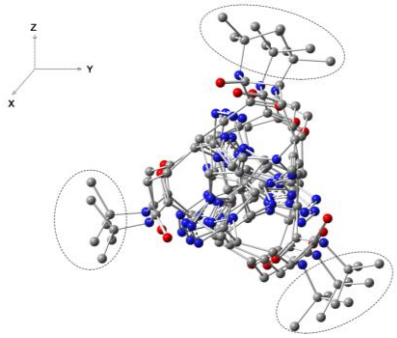

Figure 3-13. DFT-optimized conformation for the polycyclic octamer (16 monomer units) viewed from z axis (a) and side view (b). Hydrogen atoms are omitted for charity. Atoms in gray are carbon atoms, atoms in blue are nitrogen atoms; atoms in red are oxygen atoms.

3-4. Conclusions

In this chapter, an efficient and rapid synthesis strategy for the constructing of 12-membered brominated cyclic compound **13** carrying a TBDMS-protected

ethynyl group has been published. Thus, a new cyclic dimer **15** possessing azide and alkyne moieties was synthesized, and compound **15** was characterized by ^{1}H NMR, ^{13}C NMR, ESI-MS, HSQC, HMBC, and NOESY. A unique polycyclic polymer consisting of 1,4-disubstituted 1,2,3-triazole units was successfully synthesized by CuAAC polymerization of the cyclic dimer. Based on the structure of 12-membered cyclic unit, this polymer exhibits interesting helix conformation. A new dense 1,2,3-triazole alternating copolymer of *t*-Bu ester and *t*-Bu amide side chains also was synthesized by CuAAC polymerization of acyclic dimer **12.**

References

1. Badi, N.; Lutz, J. F. *Chem. Soc. Rev*. **2009**, *38*, 3383–3390.
2. Lutz, J. F. *Polym. Chem*. **2010**, *1*, 55−62.
3. Lutz, J. F.; Ouchi, M.; Liu, D. R.; Sawamoto, M. *Science* **2013**, *341*, 1238149.
4. Lutz, J. F. An Introduction to Sequence-Controlled Polymers, in Sequence-Controlled Polymers: Synthesis, Self-Assembly, and Properties. ACS Symposium Series; American Chemical Society: Washington, DC, 2014.
5. Solleder, S. C.; Schneider, R. V.; Wetzel, K. S.; Boukis, A. C.; Meier, M. A. R. *Rapid Commun*. **2017**, *38*, 1600711.
6. Meier, M. A. R.; Barner-Kowollik, C. *Adv. Mater*. **2019**, *31*, 1806027.
7. Nanjan, P.; Porel M. *Polym. Chem*. **2019**, *10*, 5406–5424.

8. LeProust, E. M.; Peck, B. J.; Spirin, K.; McCuen, H. B.; Moore, B.; Namsaraev, E.; Caruthers, M. H. *Nucleic Acids Res*., **2010**, *38*, 2522–2540.
9. Wagner, E. *Acc. Chem. Res.* **2012**, *45*, 1005–1013.
10. Trinh, T. T.; Oswald, L.; Chan-Seng, D.; Lutz, J. F. Macromol. *Rapid Commun*., **2014**, *35*, 141–145.
11. Solleder, J.-F.; Meier, M. A. R. *Angew. Chem., Int. Ed*. **2014**, *53*, 711−714.
12. Lutz, J. F. *Macromolecules*, **2015**, *48*, 4759–4767.
13. Zydziak, N.; Konrad, W.; Feist, F.; Afonin, S.; Weidner, S.; Barner-Kowollik, C. *Nat. Commun*., **2016**, *7*, 1–10.
14. Al Ouahabi, A.; Charles, L.; Lutz, J.-F. *J. Am. Chem. Soc*. **2015**, *137*, 5629–5635.
15. Leibfarth, F. A.; Johnson, J. A.; Jamison, T. F. *Proc. Natl. Acad. Sci*. **2015**, *112*, 10617–10622.
16. Barnes, J. C.; Ehrlich, D. J. C.; Gao, A. X.; Leibfarth, F. A.; Jiang, Y.; Zhou, E.; Jamison, T. F.; Johnson, J. A. *Nat. Chem*. **2015**, *7*, 810–815.
17. Porel, M.; Thornlow, D. N.; Phan, N. N.; Alabi, C. *Nat. Chem*. **2016**, *8*, 590−596.
18. Kanasty, R. L.; Vegas, A. J.; Ceo, L. M.; Maier, M.; Charisse, K.; Nair, J. K.; Langer, R.; Anderson, D. G. *Angew. Chem., Int. Ed*. **2016**, *55*, 9529−9533.

19. Jiang, Y.; Golder, M. R.; Nguyen, H. V.-T.; Wang, Y.; Zhong, M.; Barnes, J. C.; Ehrlich, D. J. C.; Johnson, J. A. *J. Am. Chem. Soc*. **2016**, *138*, 9369–9372.
20. Wicker, A. C.; Leibfarth, F. A.; Jamison, T. F. *Polym. Chem*. **2017**, *8*, 5786–5794.
21. Karamessini, D.; Poyer, S.; Charles, L.; Lutz, J. F. *Macromol. Rapid Commun*., **2017**, *38*, 1700426.
22. Brown, J. S.; Acevedo, Y. M.; He, G. D.; Freed, J. H.; Clancy, P.; Alabi, C. A. *Macromolecules* **2017**, *50*, 8731−8738.
23. Golder, M. R.; Jiang, Y.; Teichen, P. E.; Nguyen, H. V.-T.; Wang, W.; Milos, N.; Freedman, S. A.; Willard, A. P.; Johnson, J. A. *J. Am. Chem. Soc*. **2018**, *140*, 1596–1599.
24. Yang, C.; Flynn, J. P.; Niu, J. *Angew. Chem. Int. Ed*. **2018**, *57*, 16194–16199.
25. Wang, S.; Tao, Y.; Wang, J.; Tao, Y.; Wang, X. *Chem. Sci*. **2019**, *10*, 1531−1538.
26. Dong, R.; Liu, R.; Gaffney, P. R. J.; Schaepertoens, M.; Marchetti, P.; Williams, C. M.; Chen, R.; Livingston, A. G. *Nat. Chem*. **2019**, *11*, 136−145.
27. Zhao, B.; Gao, Z.G.; Zheng, Y. C.; Gao, C. *J. Am. Chem. Soc*. **2019**, *141*, 4541−4546.
28. Nanjan, P.; Jose, A.; Thurakkal, L.; Porel M. *Macromolecules* **2020** *53*, 11019–11026.

29. Laurent, E; Amalian, J. A; Parmentier, M.; Oswald, L.; Ouahabi, A. A; Dufour, F.; Launay, K. Clément, J. L.; Gigmes, D.; Delsuc, M.-A.; Charles, L.; Lutz, J. F. *Macromolecules*, **2020**, *53*, 4022−4029.
30. Yamasaki, S.; Kamon, Y.; Xu, L.; Hashidzume, A. *Polymers* **2021**, *13*, 1627.
31. Frisch, M.J.; Trucks, G.W.; Schlegel, H.B.; Scuseria, G.E.; Robb, M.A.; Cheeseman, J.R.; Scalmani, G.; Barone, V.; Mennucci, B.; Petersson, G.A., et al. Gaussian 09, Revision b.01, Wallingford CT, 2009.
32. Yang, Y.; Mori, A.; Hashidzume, A. *Polymers* **2019**, *11*, 1086.

Chapter 4

Interaction of the Dense 1,2,3-Triazole Polycyclic Polymer with Palladium Dichloride as Studied by NMR

4-1. Introduction

On the basis of noncovalent bonds including hydrogen bonding, metal–ligand interaction, dipole–dipole interaction, π–π interaction, and hydrophobic interaction, various supramolecular systems that show different dynamics from those of covalent systems have been constructed so far.[1-5] Among these noncovalent bonds, metal–ligand interaction exhibits a wide range of strengths, lengths, and dynamics depending on the combination of metals and ligands.[6,7] Therefore, a number of dynamic supramolecular systems based on metal–ligand bonds have been published.[8-22]

In the last two decades, copper(I)-catalyzed azide–alkyne cycloaddition (CuAAC), which forms 1,2,3-triazoles from azide and alkyne functionalities in the presence of copper(I) compounds, has been used in a wide variety of fields as the most important reaction in click chemistry. The importance of 1,2,3-triazole as a ligand is increasing because 1,2,3-triazole moieties act as ligand to form complexes with metal ions.[23-26] In particular, since 1,2,3-triazole functions as a ligand for palladium (Pd) ions, which can catalyze a variety of chemical reactions,

supramolecular systems based on 1,2,3-triazole–Pd have been developed. Badéche et al.[27] have synthesized 1,2,3-triazole-carrying ferrocene ligands and studied the formation of two-to-one complex of a ligand with $PdCl_2$. They reported the broader redox behavior of the complex because of the interaction of the ferrocene moieties. Wang et al.[28] have utilized 1,2,3-triazole–$PdCl_2$ coordination bonding to cross-link supramolecular polymers formed from bis(*meta*-phenylene)-[32]crown-10-based cryptand and paraquat moieties. They confirmed the formation of cross-linked supramolecular polymers by pulse-field-gradient spin-echo NMR and viscometry.

In Chapter 3, a new polycyclic polymer with a characteristic structure of 1,2,3-triazole-containing macrocycles cross-linked through 1,2,3-triazole linkages has been synthesized. This polymer can provide an environment of highly dense 1,2,3-triazole. Therefore, in this chapter, we investigate the interaction of the polycyclic polymer with Pd^{2+} ions using a mixture of the polymer and $PdCl_2$ as studied by ^{1}H NMR spectroscopy.

4-2. Materials and Methods

Materials. Palladium(II) dichloride ($PdCl_2$) was purchased from Sigma-Aldrich (St. Louis, MO, USA). Triphenylphoshine (PPh_3) was purchased from FUJIFILM Wako Pure Chemical Co. (Osaka, Japan). Other reagents were used as

received without further purification.

The polycyclic polymer sample of $M_w = 1.5 \times 10^4$ prepared in Chapter 3 was utilized.

Measurements. ^{1}H NMR measurements were carried out on a JEOL JNM ECA500 spectrometer using dimethyl sulfoxided-d_6 (DMSO-d_6) as a solvent. Chemical shifts were referenced to the residual solvent signal (2.5 ppm). Pulse-field-gradient spin-echo (PGSE) NMR data were obtained on a JEOL JNM ECA500 spectrometer at 25 °C using DMSO-d_6 as a solvent. The bipolar pulse pair stimulated echo (BPPSTE) sequence was applied.[29-31] The strength of pulsed gradients (g) was increased from 0.3 to 90 gauss cm^{-1}. The time separation of pulsed field gradients (Δ) and their duration (δ) were 0.4 and 0.002 s, respectively. The sample was not spun and the airflow was disconnected. The shape of the gradient pulse was rectangular, and its strength was varied automatically during the course of the experiments. Two-dimensional diffusion ordered spectroscopy (2D DOSY) data were obtained by inverse Laplace transformation using the SPLMOD method.[32,33]

Investigation of the interaction of the polycyclic polymer and $PdCl_2$. The sample solutions containing the polycyclic polymer and $PdCl_2$ were measured by ^{1}H NMR to study the interaction.

The polycyclic polymer sample (15 mg, 44 μmol macrocycle units) was

dissolved in DMSO-d_6 (0.45 mL). $PdCl_2$ (15.6 or 23.4 mg, 88 or 132 μmol) was added to the polymer solution. The mixture was warmed at 70 °C for 30 min to obtain a red brown transparent solution. PPh_3 (208 mg, 792 μmol) was then added to the sample solution to dissociate the complexes of the polycyclic polymer with Pd^{2+} ions.

To study the effect of the polymer concentration, sample solutions were prepared by dissolution of the polycyclic polymer (93, 123, 155 mM macrocycle units) and $PdCl_2$ (3 eq) in DMSO-d_6 with heating at 70 °C for 30 min.

To examine the effect of temperature (25, 50, 70, and 110 °C), a sample solution was also prepared by dissolution of the polycyclic polymer (186 mM macrocycle units) and $PdCl_2$ (3 eq) in DMSO-d_6 with heating at 70 °C for 30 min.

4-3. Results and Discussion

The interaction of polycyclic polymers (Figure 4-1) with $PdCl_2$ was investigated by ^{1}H NMR. Figure 4-2 displays a typical example of ^{1}H NMR spectra of mixtures of the polycyclic polymer and $PdCl_2$. In the absence of $PdCl_2$, the ^{1}H NMR spectrum for the polycyclic polymer indicates signals ascribable to the 1,2,3-triazole and methine protons at 8.3 and 6.0 ppm, respectively. In the presence of $PdCl_2$ (2 and 3 eq of the macrocycle unit), on the other hand, ^{1}H NMR spectra shows broader signals as well as new signals assignable to the 1,2,3-

triazole and methine protons at lower magnetic fields. It is likely that these new signals are ascribed to the complexes of polycyclic polymer with $PdCl_2$. The board and separated signals are indicative of the exchange between the free and complexed states which slightly slower than the time scale of ^1H NMR (~ms). When excess PPh_3 (6 eq of the macrocycle unit) was added to the mixture of polycyclic polymer and $PdCl_2$ (3 eq), the signals due to complexed species disappeared, indicating that the coordination of PPh_3 to $PdCl_2$ causes dissociation of the polymer complex.

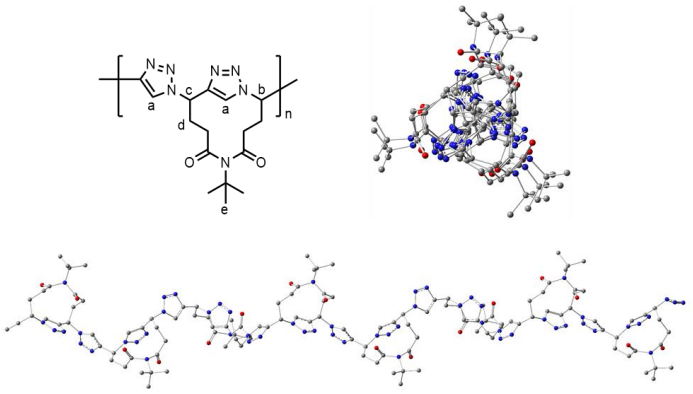

Figure 4-1. Polycyclic polymer possessing dense 1,2,3-traizole backbone and the optimized structures of polycyclic octamer (16 monomer units).

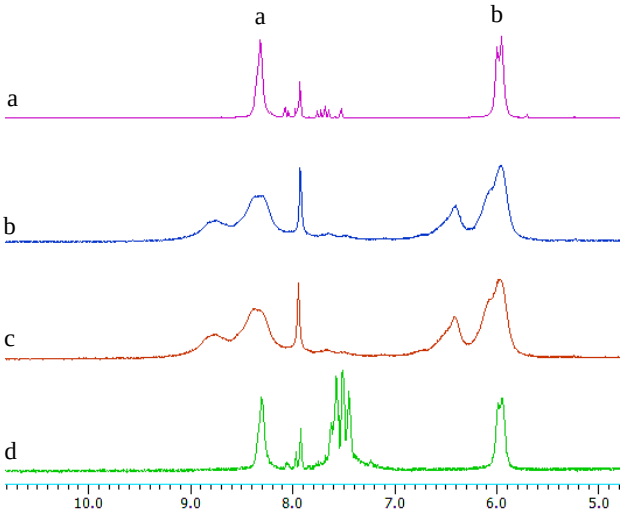

Figure 4-2. ^{1}H NMR spectra for the polycyclic polymer (98 mM macrocycles) with addition of $PdCl_2$ and PPh_3: 0 eq (a), 2 eq (b), and 3 eq of $PdCl_2$ (c), and 3 eq of $PdCl_2$ and 6 eq of PPh_3 (d) (DMSO-d_6).

To study of the conformation of polycyclic polymers in the complexed state, pulse-field-gradient spin-echo (PGSE) NMR data were obtained for the polycyclic polymer in the absence and presence of 3 eq of $PdCl_2$. Figure 4-3 compares the two-dimensional diffusion-ordered spectroscopy (2D DOSY) charts. The 2D DOSY chart in the absence of $PdCl_2$ contains all the signals due to the protons of 1,2,3-triazole, methine, two methylenes, and *t*-butyl (*t*-Bu) group. On the other hand, the 2D DOSY chart in the presence of $PdCl_2$ does not exhibit signals due to the 1,2,3-triazole and methine protons. This may be because the exchange between

the free and complexed state is slower. Using the signals of *t*-Bu group, the average diffusion coefficients were determined to be 1.9×10^{-11} and 2.8×10^{-11} $m^2\ s^{-1}$ in the absence and presence of $PdCl_2$, respectively. On the basis of Einstein–Stokes equation, the hydrodynamic radii (R_H) were calculated to be 5.3 and 3.6 nm, respectively. These data indicate that the coordination of polycyclic polymer to $PdCl_2$ did not form interpolymer cross-linking, but made the polymer take a more compact conformation.

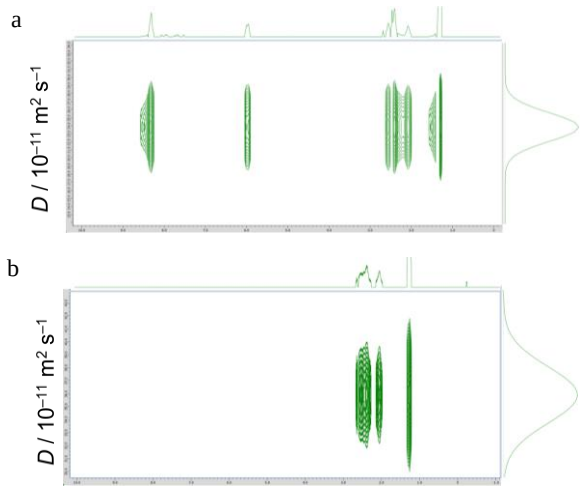

Figure 4-3. 2D DOSY spectrum for polycyclic polymer in the absence (a) and presence of 3 eq $PdCl_2$ (D_2O) (d) in DMSO-d_6.

^{1}H NMR spectra were further obtained for the mixture of polycyclic polymer and $PdCl_2$ under different conditions to study the equilibrium. Figure 4-4 shows

^{1}H NMR spectra measured for the mixture of a fixed molar ratio (3 eq of $PdCl_2$) at different concentrations. As can be seen in this figure, the signals due to the complexed state at 8.8 ppm are more significant at higher concentration, indicating that complex formation is promoted at increasing the polymer concentration. Figure 4-5 compares ^{1}H NMR spectra measured at different temperatures. As the temperature was increased, the signals due to the complexed state became less significant; Most of the polymer chains are in the free state at 110 °C. When the sample solution was cooled to 25 °C after heating, the practically same spectrum was obtained, as can be seen in Figure 4-5d. These observations indicate that the complexes formed more favorably at lower temperatures and confirm the equilibrium.

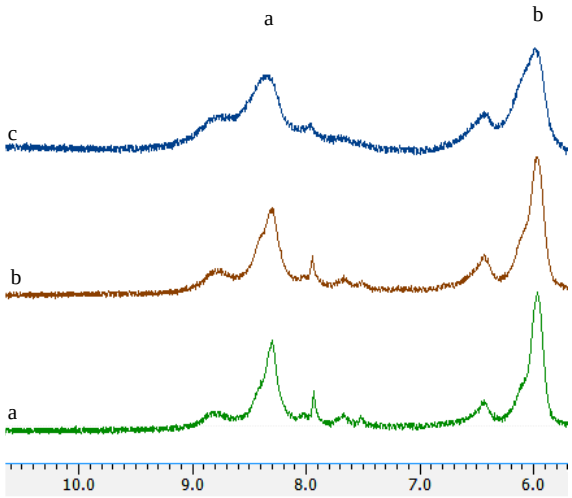

Figure 4-4. ^{1}H NMR spectra for mixtures of the polycyclic polymer (93 (a), 123 (b), and 155 mM macrocycles (c)) and $PdCl_2$ (3 eq) (DMSO-d_6).

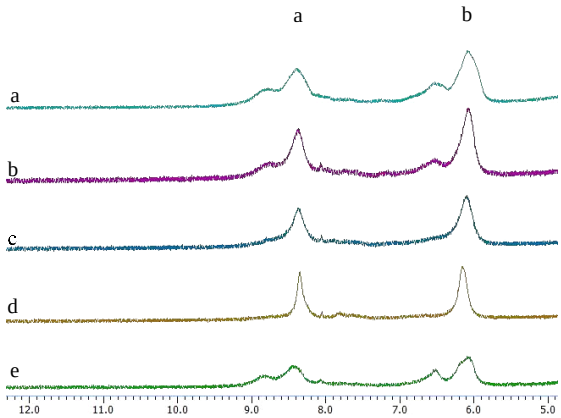

Figure 4-5. ^{1}H NMR spectra for a mixture of the polycyclic polymer (186 mM macrocycles) and $PdCl_2$ (3 eq) at 25 (a), 50 (b), 70 (c), 110 (d), and 25 °C (e, after heating) in (DMSO-d_6).

Here we assume that the 1,2,3-triazole moiety in macrocycle and $PdCl_2$ form a two-to-one complex for simplicity, it is possible to roughly estimate thermodynamic parameters for the complexation, e.g., the apparent binding constant (K_{app}), using the ^{1}H NMR data. Table 4-1 summarizes the K_{app} values estimated roughly using the area intensities of ^{1}H NMR signals due to the free and complexed states. From these data, K_{app} at 25 °C was determined to be 22 ± 4 M^{-2}. Natural logarithms of the K_{app} values were plotted in Figure 4-6 against the reciprocal absolute temperatures. This figure exhibits a good linear relationship. From the slop of straight line, the difference in Gibbs energy (ΔG) between the free and complexed states was estimated to be ca. 12 kJ mol^{-1}.

Table 1. Complexation of Polycyclic Polymer and $PdCl_2$[a]

run	temperature / °C	$C_{complex}$ [b] / mM	C_{free} [c] / mM	K_{app} / M^{-2}
1	25	30.8	67.2	26
2	50	22.7	75.3	15
3	75	18.8	79.2	11
4	110	15.1	82.9	8
5	25	26.2	71.8	19

a. The total concentrations of 1,2,3-triazole moieties in macrocycles and $PdCl_2$ were 98 and 294 mM, respectively. *b*. The concentration of complexed 1,2,3-triazole moieties. *c*. The concentration of free 1,2,3-triazole moieties.

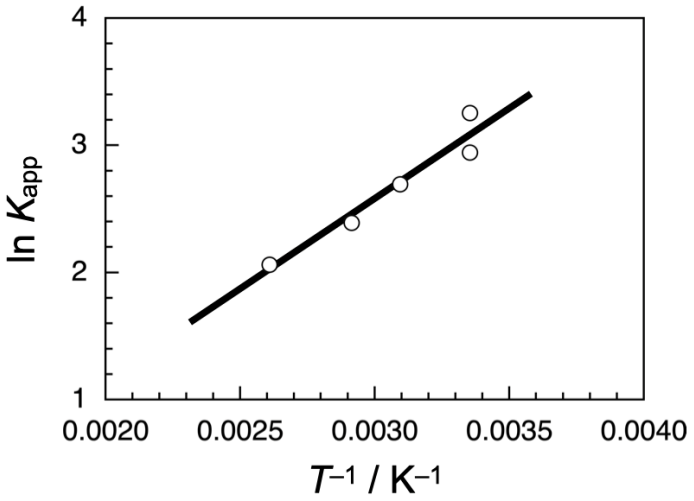

Figure 4-6. van't Hoff plot for the complexation of polycyclic polymer and $PdCl_2$.

4-4. Conclusions

The interaction of polycyclic polymers with $PdCl_2$ was investigated by ^1H NMR. In the presence of $PdCl_2$, ^1H NMR spectra shows broader signals as well as new signals assignable to the complexed 1,2,3-triazole and methine protons at lower magnetic fields. The board and separated signals are indicative of the exchange between the free and complexed states which slightly slower than the time scale of ^1H NMR (~ms). When excess PPh_3 was added to the mixture of polycyclic polymer and $PdCl_2$, the signals due to complexed species disappeared, indicating that the coordination of PPh_3 to $PdCl_2$ causes dissociation of the polymer complex. On the basis of the 2D DOSY data, the R_H values were calculated to be 9.3 and 6.3 nm, respectively, for the $PdCl_2$-free polymer and the mixture, indicating that the coordination of polycyclic polymer to $PdCl_2$ made the polymer take a more compact conformation. ^1H NMR spectra were also measured at different temperatures. As the temperature was increased, the signals due to the complexed state became less significant. Assuming that the 1,2,3-triazole moiety in macrocycle and $PdCl_2$ form a two-to-one complex for simplicity, the K_{app} values were roughly estimated. The van't Hoff plot, in which natural logarithms of the K_{app} values were plotted against the reciprocal absolute temperatures, exhibited a good linear relationship. From the slop of straight line, the difference in Gibbs energy between the free and complexed states was estimated to be ca. 12 kJ mol^{-}

[1].

References

1. Cordier, P.; Tournilhac, F.; Soulie-Ziakovic, C.; Leibler, L. *Nature* **2008**, *451*, 977–980.
2. Jiang, G.; Liu, C.; Liu, X.; Zhang, G.; Yang, M.; Liu, F.; *Macromol. Mater. Eng*. **2009**, *294*, 815–820.
3. Burattini, S.; Greenland, B. W.; Merino, D. H.; Weng, W.; Seppala, J.; Colquhoun, H. M.; Hayes, W.; Mackay, M. E.; HamLey, I. W.; Rowan, S. J. *J. Am. Chem. Soc*. **2010**, *132*, 12051–12058.
4. Wang, Q.; Mynar, J. L.; Yoshida, M.; Lee, E.; Lee, M.; Okuro, K.; Kinbara, K.; Aida, T. *Nature* **2010**, *463*, 339–343.
5. Burnworth, M.; Tang, L.; Kumpfer, J. R.; Duncan, A. J.; Beyer, F. L.; Fiore, G. L.; Rowan, S. J.; Weder, C. *Nature* **2011**, *472*, 334–337.
6. Gohy, J. *Coord. Chem. Rev.* **2009**, *253*, 2214–2225.
7. Luo, Y. R. *Comprehensive Handbook of Chemical Bond Energies, CRC Press, Boca Raton, FL, USA* **2007**.
8. Holten-Andersen, N.; Harrington, M.; Birkedal, J. H.; Lee, B. P.; Messersmith, P. B.; Lee, K. Y. C.; Waite, J. H.; *Proc. Natl. Acad. Sci. USA* **2011**, *108*, 2651–2655.
9. Andersen, A.; Chen, Y.; Birkedal, H. *Biomimetics* **2019**, *4*, 30.
10. Krogsgaard, M.; Nue, V.; Birkedal, H. *Chem.-Eur. J*. **2016**, *22*, 844–857.

11. Schmitt, C. N. Z.; Politi, Y.; Reinecke, A.; Harrington, M. J. *Biomacromolecules* **2015**, *16*, 2852–2861.
12. Mozhdehi, D.; Ayala, S.; Cromwell, O. R.; Guan, Z. *J. Am. Chem. Soc*. **2014**, *136*, 16128–16131.
13. Mozhdehi, D.; Neal, J. A.; Grindy, S. C.; Cordeau, Y.; Ayala, S.; Holten-Andersen, N.; Guan, Z. *Macromolecules* **2016**, *49*, 6310–6321.
14. Li, C. H.; Wang, C.; Keplinger, C.; Zuo, J. L.; Jin, L.; Sun, Y.; Zheng, P.; Cao, Y.; Lissel, F.; Linder, C.; You, X. Z.; Bao, Z. *Nat. Chem*. **2016**, *8*, 618–624.
15. Lai, J. C.; Li, L.; Wang, D. P.; Zhang, M. H.; Mo, S. R.; Wang, X.; Zeng, K. Y.; Li, C. H.; Jiang, Q.; You, X. Z.; Zuo, J. L. *Nat. Commun*. **2018**, *9*, 2725.
16. Götz, S.; Geitner, R.; Abend, M.; Siegmann, M.; Zechel, S.; Vitz, J.; Gräfe, S.; Schmitt, M.; Popp, J.; Hager, M. D. Schubert, U. S. *Macromol. Rapid Commun*. **2018**, *39*, 1800495.
17. Zhang, L.; Liu, Z.; Wu, X.; Guan, Q.; Chen, S.; Sun, L.; Guo, Y.; Wang, S.; Song, J.; Jeffries, E. M.; He, C.; Qing, F. L. Bao, X.; You, Z. *Adv. Mater*. **2019**, *31*, 1901402.
18. Sato, T.; Ebara, M.; Tanaka, S.; Asoh, T.-A.; Kikuchi, A.; Aoyagi, T. *Phys. Chem. Chem. Phys*. **2013**, *15*, 10628–10635.
19. Rao, Y.-L. L.; Chortos, A.; Pfattner, R.; Lissel, F.; Chiu, Y.-C. C.; Feig, V.; Xu, J.; Kurosawa, T.; Gu, X.; Wang, C.; He, M.; Chung, J. W.; Bao, Z. *J. Am. Chem. Soc*. **2016**, *138*, 6020–6027.

20. Jia, X. Y.; Mei, J. F.; Lai, J. C.; Li, C. H.; You, X. Z. *Chem. Commun.* **2015**, *51*, 8928–8930.
21. Hong, G.; Zhang, H.; Lin, Y.; Chen, Y.; Xu, Y.; Weng, W.; Xia, H. *Macromolecules* **2013**, *46*, 8649–8656.
22. Wang, L.; Di, S.; Wang, W.; Zhou, S. *RSC Adv*. **2015**, *5*, 28896–28900.
23. Suijkerbuijk, B. M. J.; Aerts, M. B. N.; Dijkstra, H. H. P.; Lutz, M.; Spek, A. L.; Koten, G.; Klein Gebbink, R. J. M. *Dalton Trans.* **2007**, 13, 1273–1276.
24. Li, Y.; Huffman, J. C.; Flood, A. H. *Chem. Commun.* **2007**, 26, 2692–2694.
25. Badeche, S.; Daran, J. C.; Ruiz, J.; Astruc, D. *Inorg. Chem*. **2008**, *47*, 4903–4908.
26. Meudtner, R. M.; Hecht, S. *Macromol. Rapid Commun*. **2008**, *29*, 347–351.
27. Badche, S.; Daran, J. C.; Ruiz, J.; Astruc, D. *Inorg. Chem.* **2008**, *47*, 4903–4908.
28. Wang, F.; Zhang, J.; Ding, X.; Dong, S.; Liu, M.; Zheng, B.; Li, S.; Wu, L.; Yu, Y.; Gibson, H. W.; Huang, F. *Angew. Chem. Int. Ed.* **2010**, *49*, 1090–1094.
29. Stejskal, E.O.; Tanner, J.E. *J. Chem. Phys.* **1965**, *42*, 288–292.
30. Tanner, J.E.; Stejskal, E.O. *J. Chem. Phys.* **1968**, *49*, 1768–1777.
31. Stilbs, P. *Prog. Nucl. Magn. Reson. Spectrosc.* **1987**, *19*, 1–45.
32. Morris, K.F.; Stilbs, P.; Johnson, C.S. *Anal. Chem.* **1994**, *66*, 211–215.
33. Huo, R.; Wehrens, R.; van Duynhoven, J.; Buydens, L.M.C. *Anal. Chim. Acta* **2003**, *490*, 231–251.

Chapter 5

Summary

In this study, new polymers possessing dense triazole backbone have been successfully synthesized by CuAAC polymerization. The structure and properties of new dense triazole polymers were systematically investigated.

In Chapter 2, a new polyanion with a dense 1,2,3-triazole backbone, poly(AH), was synthesized by CuAAC polymerization of tBuAH followed by hydrolysis of the *t*-Bu ester groups. The metal ion adsorption tests of poly(AH)Na indicated that poly(AH)Na was applicable to an adsorbent for metal ions, especially Fe^{3+} ion (98.57 ± 0.03 mg g^{-1}). The ratio of T_1 values for the ^1H NMR signals in the presence and absence of 0.6 mM Fe^{3+} indicated that Fe^{3+} ions were adsorbed more preferably onto the 1,2,3-triazole residues.

In Chapter 3, a procedure for constructing of 12-membered cyclic structure **13** has been developed by accidently. Cyclic dimer **15** was synthesized and a new polycyclic polymer (M_w = 2.0 × 10^4) possessing dense 1,2,3-triazole backbone was successfully synthesized by CuAAC polymerization of **15**. The DFT calculation indicated that the polycyclic octamer took a helical conformation presumably because of the bulky 12-membered macrocycle units. An alternating copolymer of *t*-Bu ester and *t*-Bu amide side chains was also successfully

synthesized.

In Chapter 4, the interaction of polycyclic polymers with $PdCl_2$ was investigated by ^1H NMR. In the presence of $PdCl_2$, ^1H NMR spectra showed broader signals as well as new signals assignable to the complexed 1,2,3-triazole and methine protons at lower magnetic fields. When excess PPh_3 was added to the mixture of polycyclic polymer and $PdCl_2$, the signals due to complexed species disappeared, indicating that the coordination of PPh_3 to $PdCl_2$ caused dissociation of the polymer complex. On the basis of the 2D DOSY data, the coordination of polycyclic polymer to $PdCl_2$ made the polymer take a more compact conformation. As the temperature was increased, the ^1H NMR signals due to the complexed state became less significant. Assuming that the 1,2,3-triazole moiety in macrocycle and $PdCl_2$ form a two-to-one complex for simplicity, the K_{app} values were roughly estimated. Based on the van't Hoff plot, the difference in Gibbs energy between the free and complexed states was estimated to be ca. 12 kJ mol^{-1}.

In conclusion, a new polyanion and a new polycyclic polymer possessing dense 1,2,3-triazole backbone were successfully prepared by CuAAC polymerization, and the interaction of the polyanion with metal ions and of polycyclic polymers with $PdCl_2$ were investigated. Taking advantage of unique property of 1,2,3-triazole, these polymers exhibit interesting properties. Hence, this work should provide access to new triazole-based functional materials.

List of Publications

The contents of this thesis have been published or will be published in following papers:

1. Xu, L.; Kamon, Y.; Hashidzume, A. Synthesis of a New Polyanion Possessing Dense 1,2,3-Triazole Backbone. *Polymers* **2021**, *13*, 1614. (Chapter 2)
2. Xu, L.; Kamon, Y.; Hashidzume, A. Synthesis of a Polycyclic Polymer Possessing Dense 1,2,3-Triazole Backbone. *In preparation.* (Chapters 3 and 4)

Other papers

1. Xu, L.; Wang, X.; Ma, B.; Yin, M. X.; Lin, H. X.; Dai, H. X.; Yu, J. Q. Copper mediated C–H amination with oximes: en route to primary anilines. *Chemical Science*, 2018, *9*, 5160–5163.
2. Xu, L.; Xu, H.; Lin, H. X.; Dai, H. X. Progress in the Synthesis of Primary Anilines via C–H Bond Functionalization. *Chinese Journal of Organic Chemistry*, **2018**, 38, 1940–1948.
3. Yamasaki, S.; Kamon, Y.; Xu, L.; Hashidzume, A. Synthesis of Dense 1,2,3-Triazole Polymers Soluble in Common Organic Solvents. *Polymers* **2021**, *13*, 1627.